Surface Nanostructuring for Cell and Tissue Growth

Inaugural-Dissertation

to obtain the academic degree

Doctor rerum naturalium (Dr. rer. nat.)

submitted to the Department of Biology, Chemistry and Pharmacy

of Freie Universität Berlin

by

Yulia Zhukova

from Kaliningrad, Russia

2017

This thesis is based on research conducted between February 2014 and January 2017 at the Max Planck Institute of Colloids and Interfaces, Department of Biomaterials and Freie Universität Berlin, Institute of Chemistry and Biochemistry, under the guidance of Dr. Katsiaryna Skorb.

1st Reviewer: Prof. Dr. Peter Fratzl

2nd Reviewer: Prof. Dr. Rainer Haag

Date of defense: 15th of August, 2017

Acknowledgements

First, I owe my deepest gratitude to my supervisor Dr. Katja Skorb, for constantly bringing new ideas and challenging tasks while granting me the freedom to develop my own ideas, thereby helping me to successfully move my thesis forward. Thank you for an inspiring, exciting and rewarding time!

Second, I would like to thank Prof. Dr. Peter Fratzl for giving me an opportunity to prepare my PhD thesis in the Department of Biomaterials and introducing me to the exciting field of advanced materials science. I would also like to thank Dr. John Dunlop and Prof. Dr. Helmuth Möhwald for always keeping their doors open for fruitful discussions, for sharing their precious knowledge, thereby fulfilling my experience with their scientific insights and expertise.

Moreover, I also want to thank Prof. Dr. Peter Fratzl and Prof. Dr. Rainer Haag for agreeing to review this thesis.

I am very grateful to Prof. Dr. Petra Knaus and Dr. Christian Hiepen for the fruitful collaboration with biological experiments, to Dr. Steffen Prohaska and Marc Osterland for performing computer analysis of the imaging data. Their input has been essential for achieving the scientific goals of this thesis.

Furthermore, I would like to express my gratitude to Dr. Sabine Bartosch for giving me an opportunity to be a member of the Berlin-Brandenburg School of Regenerative Therapies. Thank you for your enormous efforts managing the Graduate School, organizing numerous courses and trainings, exciting PhD Symposiums and Retreats.

I am grateful to the former and present members of the group and visiting students, namely Olga Baidukova, Svetlana Ulasevich, Nadzeya Brezhneva, Evgeny Bondarenko, Dilek Özden and Efe Yavuzsoy, for the friendly atmosphere in the lab and daily support.

I appreciate all the research facilities at the Max Planck Institute of Colloids and Interfaces and especially the technical assistants maintaining the equipment. I am very grateful to Christine Pilz-Allen for giving me hands-on experience in cell culture. Special thanks go to Anneliese Heilig, Rona Pitschke, Heike Runge, and Susann Weichold for introducing me to new microscopy techniques and performing measurements.

It was a great pleasure to work with colleagues from the Department of Biomaterials making the time at the institute enjoyable, during Klausur and Alumni meetings, conferences, and parties. And finally and most importantly, I would like to thank my family for encouraging and supporting me both in good and bad times.

Table of Contents

Summary iii

Zusammenfassung v

Introduction 7

Motivation 7

Aims and objectives 8

Outline 9

Chapter 1. Cell guidance on nanostructured metal based surfaces 11

Transition to Chapter 2 30

Chapter 2. Ultrasound-driven titanium modification with formation of surface titania based nanofoam 31

Transition to Chapter 3 41

Chapter 3. The role of titanium surface nanostructuring on preosteoblast morphology, adhesion, and migration 42

Transition to Chapter 4 56

Chapter 4. Patterned sonochemical treatment of 3D titanium scaffold with microchannels for testing the role of the first cell layer for tissue organization. 57

Abstract 57

Introduction 58

Materials and methods 60

Titanium 3D scaffolds and surface nanostructuring strategies 60

Surface characterization 61

Cell culture model 63

Microscopy and image acquisition 63

Statistical analysis 64

Results and discussion 64

Preparation and characterization of nanostructured 3D scaffolds 64

Three-dimensional tissue growth 66

Conclusion 72

Acknowledgement 72

References 72

Chapter 4: Supporting information 75

Chapter 5. General discussion 76

Back to the objectives 76

Implications of the study 77

Conclusions and perspectives 82

Publications 85
Appendices 86
Appendix 1. Ultrasonically produced porous sponge layer on titanium to guide cell behavior 86
Experimental section 96
Preparation of Nanostructured Ordered and Disordered Surfaces 96
Characterization Methods 97
Cell Culture 97
Immunofluorescent Staining 98
Gene Expression Analysis by qRT PCR 98
Statistical Analysis 99
References 99
Appendix 2. Switching the stiffness of polyelectrolyte assembly by light to control behavior of supported cells 101
Appendix 3. Methodology 112
List of Abbreviations 116
References 117

Summary

It is becoming clearer from cell biology that (nano)topographic features play an important role in cell-material interactions. Although much work has been done on the interaction between cells and idealized substrates containing nano-scaled features, it is difficult to implement such features into implant materials typically used in the clinic. For example, in the case of titanium (Ti), which is the gold standard material for load-bearing implants, a variety of surface nanostructuring techniques have been developed to improve the bioactive properties of Ti and to enhance tissue regeneration. However, most of these techniques can effectively modify only planar substrates, which limits their application for complex three-dimensional (3D) geometries of clinical implants. In this context, this thesis focuses on the application of a new surface modification strategy, which potentially allows for nanostructuring of 3D Ti scaffolds allowing the exploration of the role of nanostructures on both single cell and 3D tissue growth.

In this thesis, we investigate high intensity ultrasound (HIUS) for surface nanostructuring of titanium. This technique allows for effective modification of planar and 3D Ti surfaces through the formation of mesoporous titania (TMS) coatings on Ti suitable for biological applications. Precise control over the topographic features was achieved through the parameters of HIUS treatment such as solvent and additives, intensity, and duration of treatment. Due to its biocompatibility, physicochemical, and structural properties, TMS coating is an interesting candidate for in vitro and eventually in vivo studies.

We tested the potential of TMS surfaces in two studies, with the aim of investigating the effect of surface nanotopography on single cell behaviour and 3D tissue formation. For this purpose, we compared the cell response of the model MC3T3-E1 preosteoblast cell line on Ti surfaces with different levels of (dis)order: unmodified surface, mesoporous (TMS) and nanotubular titania (TNT) produced using anodic oxidation. The results revealed a surface-dependent shape, thickness, and spreading of cells owing to different adherence behavior. Cells were polygonal-shaped and well-spread on TMS, but elongated, fibroblast-like on TNT. Although both nanostructured surfaces impaired cell adhesion, TMS better supported cell attachment and spreading than TNT. Cell migration on TMS had a more collective character than on TNT, probably due to a closer proximity between neighboring cells. We further explored the role of nanotopography on 3D tissue growth within the microchannels of Ti scaffolds. Both external and internal surfaces of the scaffold possessed similar nanostructural features, confirming the potential of these surface treatments for modification of complex implant geometries. Although no significant differences in mean tissue layer thickness were observed on scaffolds with different nanotopography, the structure and adhesion of the tissue were affected. In contrast

to unmodified scaffolds, tissue detachment was observed on nanostructured scaffolds, indicating impaired cell adhesion.

Collectively, the studies presented in this thesis could have important implications for the design of titanium-based tissue engineering strategies and an interesting platform for lab-on-a-chip cell culturing.

Zusammenfassung

Aus der aus der Zellbiologie wird klar, dass nanotopographische Merkmale eine wichtige Rolle bei Zell-Material-Wechselwirkungen spielen. Trotz intensiver Forschungsarbeit an der Wechselwirkung zwischen Zellen und idealisierten Substraten mit nanoskaligen Eigenschaften, ist es immer noch schwierig diese Eigenschaften auf gängige Implantatmaterialen zu übertragen. Beispielsweise wurde für Titan, dem Goldstandard für lasttragende Implantate, eine Vielzahl von Oberflächen-Nanostrukturierungsverfahren entwickelt. Die durch diese Verfahren hergestellten Oberflächen verbessern nachweislich die bioaktiven Eigenschaften von Titan und beschleunigen die Heilung und Geweberegeneration. Allerdings können durch die meisten dieser Techniken nur planare Oberflächen effektiv modifiziert werden, was ihre Anwendung für komplexe dreidimensionale (3D) Geometrien von klinischen Implantaten limitiert. Aus diesem Grund konzentriert sich diese Dissertation auf die Anwendung einer neuen Oberflächenmodifikationsstrategie, die potenziell auch die Nanostrukturierung von 3D-Titangerüsten ermöglicht, und damit die Erforschung der Rolle von Nanostrukturen sowohl im Einzelzell- als auch im 3D-Gewebewachstum ermöglicht.

In dieser Dissertation untersuchen wir eine neue Methode zur Titan-Oberflächen-Nanostrukturierung mit hochintensivem Ultraschall (HIUS). Diese Technik ermöglicht eine effektive Modifizierung von planaren und dreidimensionalen Titanoberflächen. Die erzeugten mesoporösen Titanoxidoberflächen (TMS) eignen sich hervorragend für biologische Anwendung. Die HIUS-Behandlung ist eine ideale Methode für die Meso-Strukturierung von Feststoffen, mit der man die topographischen Eigenschaften der produzierten Oberflächen durch Parameter wie dem Lösungsmittel, die verwendeten Zusatzstoffe, der Intensität und der Dauer des Ultraschalls präzise bestimmen kann. Mesoporöses Titandioxid erscheint aufgrund seiner Biokompatibilität sowie seiner physikochemischen und strukturellen Eigenschaften auch für weitere *in vitro* und eventuell auch *in vivo* Studien sehr gut geeignet zu sein.

Im Rahmen dieser Dissertation wurde die Auswirkung von verschiedenen TMS-Oberflächen auf das Zellwachstum in zwei verschiedenen Experimenten untersucht. Zunächst wurde die Wirkung der Oberflächen-Nanotopographie auf das Einzelzellverhalten untersucht und im zweiten Schritt auf die 3D-Gewebebildung. Zu diesem Zweck untersuchten wir das Verhalten von Modell-MC3T3-E1-Präosteoblasten-Zellinien auf Titanoberflächen mit unterschiedlichen Unordnungsgraden: unmodifiziertes Titan, mesoporöses- (TMS) und nanotubuläres- Titanoxid (TNT) hergestellt durch anodische Oxidation. Die Ergebnisse zeigten eine oberflächenabhängige Form, Dicke und Ausbreitung von Zellen aufgrund unterschiedlicher Adhäsion. Die Zellen auf TMS waren polygonal geformt und gleichmäßig auf der Oberfläche

verteilt, dagegen waren die Zellen auf TNT langgestreckt und fibroblast-artig. Obwohl beide nanostrukturierte Oberflächen die Zelladhäsion verschlechterten, erfolgte die Anlagerung und Ausbreitung von Zellen auf TMS besser als auf TNT. Die Zellmigration auf TMS hatte einen kollektiveren Charakter als auf TNT, wahrscheinlich infolge des geringeren Abstandes zwischen benachbarten Zellen. Darüber hinaus haben wir die Rolle der Nanotopographie auf das 3D-Gewebewachstum in den Mikrokanälen von Titangerüsten untersucht. Sowohl die Außen- als auch die Innenfläche des Gerüstes besaßen ähnliche nanostrukturelle Merkmale und bestätigten das Potential dieser Oberflächenbehandlungen zur Modifikation komplexer Implantatgeometrien. Obwohl keine signifikanten Unterschiede in der mittleren Gewebeschichtdicke von Gerüsten mit unterschiedlicher Nanotopographie beobachtet wurde, wurden die Struktur und die Adhäsion des Gewebes auf der Oberfläche beeinflusst. Im Gegensatz zu nichtmodifizierten Gerüsten wurde bei nanostrukturierten Gerüsten eine Gewebeablösung beobachtet, was auf eine verminderte Zelladhäsion hindeutet.

Zusammengefasst könnten die in dieser Dissertation vorgestellten Experimente wichtige Erkenntnisse für das Design von titanbasierten Gewebe- Engineering-Strategien und eine interessante Plattform für die Lab-on-a-Chip-Zellkultivierung haben.

Introduction

Motivation

Titanium and titanium alloys are widely used in biomedical applications, such as hard tissue replacements[1-3] in bone, joint, and dental implants,[4] as well as in cardiac and cardiovascular implants. Titanium represents a gold standard in implantology due to its lower elastic modulus, better corrosion resistance, and superior biocompatibility when compared to stainless steel and cobalt alloys. However, titanium and its alloys cannot meet all of the clinical requirements. Bioinert materials, such as titanium, are used for hard tissue replacements, since they are stable in the human body and does not react with body fluids, thereby minimising adverse tissue reactions. This is achieved by the encapsulation of the bioinert material into the living body by fibrous tissues that isolate them from the surrounding. Therefore, it is still difficult to achieve good chemical bonding of titanium with bones and form new bones on its surface at the early stage of implantation. In addition, young patents requiring implants and growing human life expectancy have driven biomedical research to reconsider the requiremens to titanium implants. Original implant concerns, such as materials strength, infection, and short-term rejection are currently reconsidered to more long-term issues, such as wear, fatigue strength, and long-term biocompatibility.[1]

Due to our improved understanding of the native extracellular environment, it is now recognized that material-host tissue interactions are strongly influenced by nanometric surface cues. This is perhaps not surprising as: (1) cells grow on nanostructured extracellular matrices; (2) adsorbed proteins and their aggregates have nanodimensions; and (3) biological events such as signalling occur at the nanometric level. As a consequence, multiple efforts have led to the development of metal-based materials with modified nanotopography, aiming to regulate cell performance on implant relevant biomaterials. Progress in nanotechnology now makes it possible to precisely design and modulate the surface properties of implant-relevant materials at the nanoscale. Nanoengineered surfaces possess the unique capacity of directly affecting both molecular and cellular events, which determine the overall biological response to the implanted material, such as protein adsorption, cell adhesion, proliferation, etc.

Due to its inertness, corrosion resistance and high mechanical strength, titanium is very difficult to modify. To date, various strategies have been developed to generate nanoscale surface features on titanium-based materials, such as acid- and alkali etching, anodic oxidation, laser treatments, etc. However, the majority of the titanium surface nanostructuring techniques are expensive, time-consuming or could not be applied for large scale implant production, thereby

not offering a clinical applicability. A number of challenges should be addressed for defined surface nanostructuring and surface characterization. For example, the specifics of the nanostructuring processes resulting in the formation of porous surfaces in 2D is poorly understood, let alone in 3D. A potential advantage of using nanostructuring is the ability to avoid additional surface coating with polymers or ceramics in order to enable the direct contact of tissue with the metal or metal oxide. Therefore, it is necessary to develop novel methods allowing straight-forward nanomodification of titanium implants with complex geometries. Moreover, the majority of *in vitro* studies aiming to investigate the effect of nanotopography on cell behaviour are performed on planar two-dimensional (2D) titanium specimens, which do not allow to answer the question how nanotopography affects three-dimensional (3D) tissue formation. The functional properties of tissues arise through the interactions of numerous cell types.[5-6] *In vivo*, these interactions occur in a 3D setting in the context of specific tissue structures. Tissue structure is defined as tissue size, shape, composition, spatial heterogeneity, and the surrounding ECM. Such 3D structure has an important role in the exchange of chemical, electrical and mechanical signals within the tissue. Therefore, it is important to study cell-nanotopography interactions in the 3D model system.[7] The *in vivo* studies have however limitations, since they mostly provide only the final observations of the implants osseointegration level, but do not bring attention to the first cell layer in contact with the implant surface. Therefore, the mechanism and duration of the nanotopography effect on tissue growth still remain unclear.

In this thesis, we propose a new platform for titanium surface nanostructuring, which allows for effective scalable modification of Ti surface and furthermore allows a more systematic investigation of the effect of surface nanotopography on single cell behaviour in 2D as well as on 3D tissue formation.

Aims and objectives

This doctoral thesis presents an interdisciplinary research project, which combines the studies from two disciplines: materials science and biology.

First, this thesis further extends HIUS, a sonochemical method of metal nanostructuring developed by Skorb and co-workers by fabricating superhydrophilic, bio- and cytocompatible mesoporous titania surfaces for cell culture. Due to its mechanical strength and inertness, titanium has been widely used as a biomaterial for various medical applications, these properties however make titanium a difficult material to modify. Moreover, a lot of engineering efforts are required to develop a scalable technology for implant nanomodification. The

majority of metal surface (nano)structuring/patterning techniques presented in literature are suitable only for laboratory conditions. In contrast, the method presented in this thesis is a potentially industrially scalable process depending on the area of the metal surface to be treated as per manufacturer's information.[8] The upscaling of the process can be achieved by using special arrangements of multiple ultrasonic devices.[9] Therefore, the sonochemical method of titanium surface nanostructuring is potentially suitable for clinical applications.

Second, this thesis explores how physical patterning of titanium surface in absence of (bio)chemical stimuli affects cell behaviour. In this context, this doctoral thesis aims to investigate cell and tissue growth at different stages and to answer the following questions:

(1) how surface nanotopography affects cell growth at early stages after seeding;
(2) how surface nanotopography plays a role in later stages of tissue formation in 3D systems.

Two-dimensional cell growth on surfaces with modified topography has been often shown in literature. For example, the nanotopographic control of cell behaviour has been recently addressed in the study by Kopf *et al.*[10] in collaboration with the Biochemistry group from Freie Universität Berlin, where C2C12 cell response to mesoporous titania produced by our method has been investigated. In the Biomaterials Department at the MPIKG there is extensive experience with the mouse osteoblastic cell line MC3T3-E1, especially in the large-scale cell culture experiments in the group of Dr. John Dunlop. Therefore, to study the effect of surface nanotopography on cell behaviour, we chose to use MC3T3-E1 preosteoblasts in our experiments in order to best compare the results to existing data. Finally, we aim to apply the acquired knowledge of early-stage cell-nanotopography interactions to later stages of tissue growth, i.e. from 2D to 3D systems.

Outline

This thesis is made up of four publications: two accepted for publication, one submitted and one in preparation. In addition, I am a co-author in two more publications provided in Appendices 1 and 2.

The first article presents a literature review of methods for metal surface nanostructuring for bioapplications. The review article further summarises the effects of metal surface nanotopography on cell behaviour (Chapter 1). In addition, this paper provides examples of stimuli-responsive metal-based polyelectrolyte systems developed due to the photoactive properties of titanium via nanostructuring. In this publication, the state-of-art was analyzed and future prospects in the area of metal surface nanostructuring for bioapplications were discussed.

The second article presents the method of sonochemical formation of surface titania nanofoam under high intensity ultrasound treatment in alkaline solution (Chapter 2). Mesoporous titania surfaces formed by this technique possess a specific surface nanotopography, defined as random, sponge-like titania with nanoscale surface roughness and porosity with an average pore diameter of approx. 70 nm, and superhydrophilic. Mesoporous titania is also bio- and cytocompatible as shown with a MC3T3-T1 preosteoblast cell culture model. This publication not only contributes to the understanding of the mechanisms involved in titanium surface modification with HIUS in alkali solution, but also demonstrates the prospects of this method for cell culturing.

The third article demonstrates the effect of titanium surface nanotopography on preosteoblast morphology, adhesion and migration (Chapter 3). To investigate the relationship between surface nanotopography and cell behaviour, the cell response to ordered and disordered nanotopographies is compared. Nanotubular titania surfaces fabricated by well-established electrochemical method are used as model “ordered” nanotopographies, and mesoporous titania described in Chapter 2 is used as a model for disordered nanotopography. This paper shows distinctly different cell behaviours on ordered and disordered titania surfaces, thereby indicating the role of surface nanotopography for the modulation of cell behaviour.

The fourth article (Chapter 4) demonstrates the application of sonochemical and electrochemical methods for the nanostructuring of microchannels of tissue engineering scaffolds. In contrast to studies in Chapter 3, investigating early cell response to nanotopography, the scaffolds are used to study effect of nanotopography on later stages of tissue growth in 3D. This publication provides evidence that these methods can be applied to modify the surfaces of complex geometries, as well as proposes a new approach to answer the fundamental question: how long surface nanotopogaphy plays a role in cell/tissue growth.

The final section of this thesis (Chapter 5) provides the discussion of the individual articles and summarizes their main conclusions into the general context.

Chapter 1. Cell guidance on nanostructured metal based surfaces

Yulia Zhukova, Ekaterina V. Skorb*

Max Planck Institute of Colloids and Interfaces, Am Mühlenberg 1, Potsdam 14424, Germany

* Corresponding author

This manuscript is published in Advanced Healthcare Materials: Adv. Healthcare Mater. 2017, 1600914.

My Contribution: I participated in the elaboration of the structure of the review, contributed to the literature research, made 4 figures, and co-wrote the manuscript with another author.

http://dx.doi.org/10.1002/adhm.201600914

Transition to Chapter 2

In Chapter 1 we provided a comprehensive introduction into nanostructured metal-based functional systems. To date there have been many studies on metal surface nanostructuring, in particular using sonochemical treatment as the preceding review chapter shows. In the last decade, it was demonstrated that a metal matrix produced by the sonochemical method could be effectively used for the construction of hybrid materials[11-12] and surface encapsulation systems.[13-15] Different metals such as aluminium, their alloys and steel could serve as metal matrices, when treated with HIUS.[16] Moreover, several studies reported construction of intelligent metal-based encapsulation systems consisting of the sonogenerated porous metal surface and polyelectrolyte multi-layered coatings. For example, Andreeva *et al.*[17] reported an upload, storage and controlled pH-triggered release of an anti-cancer drug doxorubicin out of sonochemically formed surface metal sponges. Further applications of metal-polymer systems include anticorrosive,[17-19] antibacterial,[20-21] and drug delivery [17] These studies suggest that such biocomposite materials, in particular sonogenerated mesoporous titania, have a bioapplication potential. Therefore, the study presented in Chapter 2 aimed to use HIUS for the modification of titanium and to identify optimal processing conditions for the production of mesoporous titania surfaces suitable for cell culturing. To investigate the mechanism of mesoporous titania formation, we characterised the relationship between the surface morphology and physicochemical properties, i.e. roughness and hydrophilicity. Finally, this chapter discusses the implications of this study on future applications of sonogenerated mesoporous titania surfaces to study cell-nanotopography interactions.

Chapter 2. Ultrasound-driven titanium modification with formation of surface titania based nanofoam

Yulia Zhukova,* Sviatlana A. Ulasevich, John W. C. Dunlop, Peter Fratzl, Helmuth Möhwald, Ekaterina V. Skorb

Max Planck Institute of Colloids and Interfaces, Am Mühlenberg 1, 14424 Potsdam, Germany

* Corresponding author

This publication is published in Ultrasonics Sonochemistry: Ultrasonics Sonochemistry 36 (2017) 146 – 154. DOI: 10.1016/j.ultsonch.2016.11.014.

My Contribution: I performed titanium surface nanostructuring, surface characterization (AFM, contact angle measurements), and cell culture experiments; analysed the data on surface roughness and contact angle values and cell proliferation; and wrote the manuscript.

http://dx.doi.org/10.1016/j.ultsonch.2016.11.014

Transition to Chapter 3

Chapter 2 demonstrated a novel method for the *in situ* production of the mesoporous titania coating by HIUS treatment in alkali solution. Optimal processing parameters were identified to produce highly hydrophilic mesoporous titania with nanoscale surface roughness. Moreover, the mesoporous titania layer on bulk titanium was shown to be interpenetrating from surface to bulk, providing high bonding strength to bulk metal. Furthermore, this surface presented good cytocompatibility to a preosteoblast cell line. Taken together, these findings indicate that mesoporous titania performs well across two surfaces: between bulk metal and nanostructured surface, and between nanostructured surface and the tissue, thereby suggesting potential applications of mesoporous titania surfaces in biological studies.

Having found a straight-forward approach for the sonochemical-based production of cytocompatible nanostructured titania, we were prompted to further study cell-nanotopography interactions. In the study presented in Chapter 3 we aimed to identify and characterize the cell-nanotopography interactions on nanostructured titania surfaces. To investigate the role of surface nanotopography on cell behaviour, we compared the cell response to ordered (nanotubular) and disordered (mesoporous) titania nanotopographies. In the study presented in Chapter 3, MC3T3-E1 preosteoblasts were used as an *in vitro* cell culture model, and cell behaviour (proliferation, morphology, adhesion, and migration) was analysed at early stages after seeding. The scratch wound healing assay was performed for the estimation of cell migration characteristics on mesoporous and nanotubular titania surfaces. Finally, we discuss the implications of early-stage cell adhesion on later stages of thick tissue growth since we think there is a crucial role of the first cell layer in further tissue formation. This study is based on our recent work by Kopf *et al.*[10](Appendix 1), where we compared an impact of these nanotopographies on C2C12 cell behaviour. To our knowledge, our paper[10] was the first study to compare cell response on mesoporous and nanotubular titania surfaces.

Chapter 3. The role of titanium surface nanostructuring on preosteoblast morphology, adhesion, and migration

Yulia Zhukova,[1‡] Christian Hiepen,[2‡] Petra Knaus,[2] Marc Osterland,[3,4] Steffen Prohaska,[4] John W. C. Dunlop,[1] Peter Fratzl,[1*] Ekaterina V. Skorb[1]

[1] Department of Biomaterials, Max Planck Institute of Colloids and Interfaces, 14476 Potsdam-Golm, Germany

[2] Institute for Chemistry and Biochemistry, Freie Universität Berlin, 14195 Berlin, Germany

[3] Zuse Institute Berlin, 14195 Berlin, Germany; Institute for Mathematics, Freie Universität Berlin, 14195 Berlin, Germany

[4] Zuse Institute Berlin, 14195 Berlin, Germany

* Corresponding author

[‡] The authors contributed equally to this publication.

This manuscript is accepted in Advanced Healthcare Materials.

My Contribution: I performed (1) titanium surface nanostructuring with sonochemical treatment and anodic oxidation; (2) surface characterization: surface roughness measurement with AFM and contact angle measurements and the corresponding data analysis; (3) cell culture experiments: MC3T3-E1 cell cultivation, cell imaging by means of phase contrast and confocal laser scanning microscopy, (immuno)fluorescent stainings for the visualization/estimation of cell morphology and adhesion, analysed the data on cell attachment, cell morphology, cell adhesion, and on Ki67 cell proliferation assay. I made Figures 1 – 5, Supporting Information Figures 1 – 6 and wrote the manuscript.

http://dx.doi.org/10.1002/adhm.201601244

Transition to Chapter 4

The study presented in Chapter 3 investigated the effect of titania surface nanotopography on the early-stage response of MC3T3-E1 preosteoblasts, such as cell attachment, morphology, adhesion and migration. Cytocompatibility of mesoporous titania shown in Chapter 2 was further confirmed and compared to well-studied nanotubular titania highlighting the role of surface (dis)order on cell behaviour. First, cell morphology was strongly affected by nanotopography: a polygonal cell shape and spreading was observed on mesoporous titania in contrast to more elongated polarized cell shapes on nanotubular titania. It was shown that cell proliferation, morphology, and adhesion were strongly affected by nanotubular titania surface. This could be due to possible differences in protein adsorption on the different surfaces that prevent integrin clustering on nanotubular titania. Alternatively, the low contact angle of mesoporous titania as well as of nanotubular titania might have diminished cell adhesion on nanostructuring surfaces. Moreover, nanotopography modulates migratory cell behaviour and is affected by cell morphology and adhesion. In addition to the observations made at early stages directly after cell attachment, we found differences in cell density on nanotopographies at later stages of tissue growth. These data provide first evidence that nanotopography alters not only the behaviour of individual cells, but also of the thicker tissue at later stages.

Based on these findings, we asked whether the behaviour of the first cell layer plays an essential role in thick tissue formation. To answer this question, we perform nanostructuring in the microchannels of the 3D titanium scaffolds and measure the rate of tissue growth inside the microchannels. The results are presented in the following chapter. There have been many studies on understanding 3D tissue growth in channels of different geometries. Previously, Rumpler *et al.* [22-23] and Bidan *et al.* [24-25] reported that tissue growth could be described by a model for curvature-controlled growth. However, we hypothesize that tissue growth could be controlled not only by tuning the geometry of the tissue engineering scaffolds at macro scale, but also by nanoscale topographies. In final Chapter 5, we discuss the implications of our findings on current thinking in the field of cell biology.

Chapter 4. Patterned sonochemical treatment of 3D titanium scaffold with microchannels for testing the role of the first cell layer for tissue organization.

Yulia Zhukova, Olga Baidukova, John W. C. Dunlop, Peter Fratzl, Ekaterina V. Skorb*

Am Mühlenberg 1, 14424 Potsdam, Germany

* Corresponding author

This manuscript is in preparation.

My Contribution: I performed surface nanostructuring of the 3D tissue engineering scaffolds, cell culture experiments, image acquisition by means of phase contrast microscopy and confocal laser scanning microscopy. I analysed the data on nanopore arrangement on nanostructured surfaces, and projected tissue area and wrote the manuscript.

Abstract

Titanium osseointegration is critical for the successful performance of dental and orthopedic implants. Previous studies have shown that surface structural modifications at the nanometer scale affect mechanical and biological properties of titanium-based implants and enhance their healing and tissue repair abilities. The aim of the present study was to develop a simple and scalable sonogenerated surface modification treatment that introduces nanoscale features to both plane and shaped Ti-based scaffolds for tissue engineering, and to determine how long the adhesion of the initial cell layer plays a role in 3D tissue formation in the absence of any exogenous soluble factors. A simple sonochemical treatment was for the first time applied for generating controlled mesoporous (TMS) nanotopographies on 3D Ti scaffolds with microchannels. Moreover, the HIUS treatment was also applied for spatially regulated modification with surface patterning. MC3T3-E1 cells were seeded on unmodified and modified 3D Ti scaffolds. Superimposition of nanostructures to the tissue scaffolds strongly affected the behaviour of both the first cell layer and 3D tissue behaviour. The results suggested that the tissue formation rate, structure, and its detachment in the microchannels of the scaffolds could be affected by surface nanotopography, with important implications towards the understanding of nanotopography effect on tissue formation as well as towards the scaffold design for improved implant osseintegration *in vivo*.

Keywords: titanium; nanotopography; tissue engineering scaffold; microchannel; three-dimensional tissue formation; osteoblasts

Introduction

Titanium (Ti) osseointegration is critical for successful tissue regeneration in dental and orthopaedic applications. Due to its mechanical strength and inertness, titanium and its alloys has been widely used for the production of dental and orthopedic implants.[1-5] These properties however make titanium a difficult material to modify and a lot of engineering efforts are required to develop a scalable technology for implant nanomodification. Titanium surface nanomodifications include different techniques, divided into three groups, such as mechanical (e.g., polishing, machining, blasting), chemical (e.g., anodic oxidation,[6] acid-etching, alkali-etching), and physical (e.g., plasma spray treatment,[7] ion implantation,[8] laser treatments[9]).[1] The chemical surface treatments are very effective due to their simplicity and homogeneous modification of the substrate due to the uniform access of the reactive solution to the surface. However, the majority of the previous studies reported the nanostructuring on plane titanium surface and are suitable only for laboratory conditions. Only a few studies reported titanium nanostructuring on complex implant geometries,[10-13] indicating that the majority of these methods cannot be applied for surface nanostructuring of the implant-relevant devices with complex geometries. The sonochemical treatment proposed in this study is a potentially industrially scalable process. The upscaling of the process can be achieved by using special arrangements of multiple ultrasonic devices as was shown for the applications in food industry.[14] As per manufacturer's information,[15] by using the similar approach the process upscaling can be achieved also for other applications, such as metal surface modification, by aligning multiple ultrasonic devices with respect to the area of the metal surface to be treated. Therefore, we propose a novel sonochemical treatment, which provides the formation of mesoporous titania surface layer and can potentially be applied for modification of titanium scaffolds with complex geometries for tissue engineering and implant applications.

In this study, high intensity ultrasound (HIUS) in combination with alkali treatment[16-17] was used to provide homogeneous nanostructuring of the inner surfaces of simple porous titanium scaffolds. We have recently reported that this novel sonochemical method can be applied to fabricate mesoporous titania (TMS) surfaces.[18] Moreover, due to its hydrophilicity and biocompatibility, TMS can be used for bioapplications. For comparison, we use a well-studied electrochemical method – anodic oxidation, which allows fabricating nanotubular titania (TNT) surfaces.[19--20] Similar to other nanostructuring methods, the majority of surface engineering

and *in vitro* studies were performed on plane titanium. We for the first time show the proposed sonochemical treatment for nanostructuring of the inner surfaces of scaffolds' microchannels.

To date, several fundamental studies suggest the role of surface nanotopography on cell growth (please refer to Review[21]). Titanium surface nanomodification of dental and orthopedic implants is a common approach to enhance osseointegration.[22-23] Multiple observations show the effect of titanium surface nanotopography and porosity on early-stage cell behavior, from single cells up to confluent single-cell layers. However, monolayer, or 2D, cell cultures do not adequately mimic the cellular environment in the living tissue. Within a tissue, cells interact with each other and with the extracellular matrix (ECM), forming cell-cell and cell-matrix interactions, respectively. These interactions establish a 3D communication network through biochemical and mechanical cues.[24] Therefore, development of the *in vitro* 3D systems providing more accurate depiction of physiological cell-cell and cell-matrix interactions is necessary. For example, the 3D composite polymer-based scaffolds with controlled micro- and nanotopographical features were fabricated by the 3D-printing to better mimic ECM architecture. Due to the surface decoration with TiO_2 and bioactive glass nanoparticles, the 3D scaffolds were shown to enhance MC3T3-E1 cell response. [25] Moreover, the shape-shifting polymer materials are of special interest for creating 3D cell culture systems, since they are programmed for 2D to 3D transformations in shape and functionality like in natural events. [26] Therefore, in this study, our goal is to investigate the role of surface nanotopography on tissue formation in the 3D cellular environment. For this purpose, we use the 3D scaffold design previously demonstrated in 3D culture of MC3T3-E1 preosteoblasts.[27] These cells were seeded on 3D hydroxyapatite (HA) scaffolds containing channels of different shapes (triangular, square, hexagonal, and round) and sizes produced by rapid prototyping. Such scaffold design allows formation of thick tissues with cells and ECM highly organized with respect to the scaffold geometry. Moreover, the rate of tissue growth was found to be controlled in a curvature dependent manner.[28] In the works of Rumpler *et al* [27] and Bidan *et al*,[29] HA was chosen as a substrate material, since HA is known to support the formation of bone tissue. MC3T3-E1 cells were chosen as a model system, since they are known (1) to undergo differentiation from an immature preosteoblastic to a mature osteoblastic phenotype *in vitro*[30] and (2) to build an extracellular matrix of well-organized collagen fibrils and non-collageneous matrix proteins known from bone tissue.[31] In the following we use the similar geometries made in Ti to enable metal surface nanostructuring of the surfaces of the 3D scaffolds.

Using HIUS method for surface nanostructuring (shown on plane surface in Chapter 2), the present study aims to: (1) modify 3D Ti scaffold with microchannels for 3D tissue growth, and (2) perform spatially regulated modification with surface patterning. For comparison to HIUS,

we used classical anodization technique. The first goal of the present study is to test whether effective titanium modification can be achieved by sonochemical treatment in the microchannels of the 3D scaffold. We have superimposed nanostructures on Ti 3D tissue engineering scaffolds and examined the 3D tissue formation in the microchannels of the scaffolds.

Besides the practical interest for engineering, such scaffolds are necessary for answering the question how important the first cell layer for tissue organization is. Regulation of the cell adhesion by using nanostructured titania surfaces was shown in Chapters 2 and 3. However, only first layer interacts with surface, whereas further tissue layers are probably not affected by surface nanotopography. We hypothesize that at later stages of tissue growth the surface nanotopography is still important. Therefore, the next goal is to test the hypothesis that nanotopography-modified first cell layer can affect the 3D tissue formation in the absence of any exogenous soluble factors. To test this hypothesis, patterned substrates were fabricated where one part of the scaffold was modified, whereas another part was left unmodified due to masking. In this way, we initially program the scaffold to induce the first cell layer forming more focal contact points on the unmodified part and less focal contacts on the nanostructured part.

Materials and methods

The experimental protocol is shown in **Figure 1**.

Titanium 3D scaffolds and surface nanostructuring strategies

Titanium foil (1 mm thick) was cut into the plates (1 x 2 cm) to fit the homemade Teflon sample holder used for sonication. For the production of one scaffold, one titanium plate (1 x 2 cm) was cut into two parts (0.5 x 2 cm each), and 9 square open microchannels (500 x 500 µm) were made on one side of one part. Two parts of the scaffold are held together by a Teflon frame (**Figure S1**). This construction allows observation of nanotopography and tissue formation inside the microchannels. Prior to nanostructuring, each part of the scaffold was chemically polished in the solution of HNO_3 (66.7 vol. %) and HF (33.3 vol. %). For the cell culture studies, the scaffolds with microchannels of different shape (triangular, square, round) and size (500 µm) were prepared.

In total, two surface modifications were used: mesoporous Ti (TMS) andtitanium nanotubes (TNT). TNT was used for the comparison with TMS (for details see Chapter 3). For the production of TMS samples, titanium scaffolds were ultrasonically treated for 10 min in presence of 5M NaOH using the ultrasonic processor UIP1000hd (Hielscher Ultrasonics

GmbH, Germany) with a maximum output power of 1000 W. The apparatus was equipped with a sonotrode BS2d18 (head area 2.5 cm^2) and booster B2-2.2, magnifying the working amplitude in 2.2 times. Sonication was performed at 19.8 kHz and constant temperature of around 333 K monitored by the thermo sensor inserted into the working solution of NaOH. For the production of TNT samples, titanium scaffolds were anodized in an aqueous solution of ethylene glycol (2 vol. % water) containing 0.75 wt. % NH4F. At beginning of the anodizing, potential linearly increased from 0 to 40 V, then the anodizing performed at potentiostatic (40 V) mode for 20 min. All samples were additionally rinsed with ethanol and water and heat treated at 450 °C in the oven for at least 3 hours. Several washing steps and thermal treatment allow a complete elimination of the working solutions, which could have a negative effect on cell growth. Milli-Q water (18 MΩ·cm) was used in all aqueous solutions. Untreated titanium was used as a control.

To confirm the "non-line-of-sight" nature of the nanomodification induced by sonochemical and electrochemical treatments, the 3D scaffolds of with microchannels of complex shape had been first exposed to the metal polishing solution (2 volume parts HNO3, 1 volume part HF), followed by one of the nanomodification treatments described above. The nanotopography generated on the internal walls of the scaffold was compared to those generated on the external plane surface of the scaffold.

Surface characterization

Electron microscopy

Surface nanotopography was qualitatively evaluated using a scanning electron microscope (SEM, Gemini Leo 1550) with an operating voltage of 3 keV. Histograms of the nanopore diameters of TMS and TNT were generated with the image analysis software ImageJ (NIH, USA) using three fields of view from two different samples per surface type, with at least 150 nanopores per micrograph. In addition, the thickness and structure of the oxide layer formed upon the sonochemical treatment was evaluated using a transmission electron microscope (TEM, Zeiss EM 912 Omega, Carl Zeiss AG, Germany) operated at 300 kV and equipped with an electron-diffraction (ED) unit. High-resolution transmission electron microscopy (HRTEM) was performed by TEM in a Philips CM30 operated at 300 kV. The samples were ultramicrotomed (Leica EM FC6) and placed onto carbon-coated copper grids.

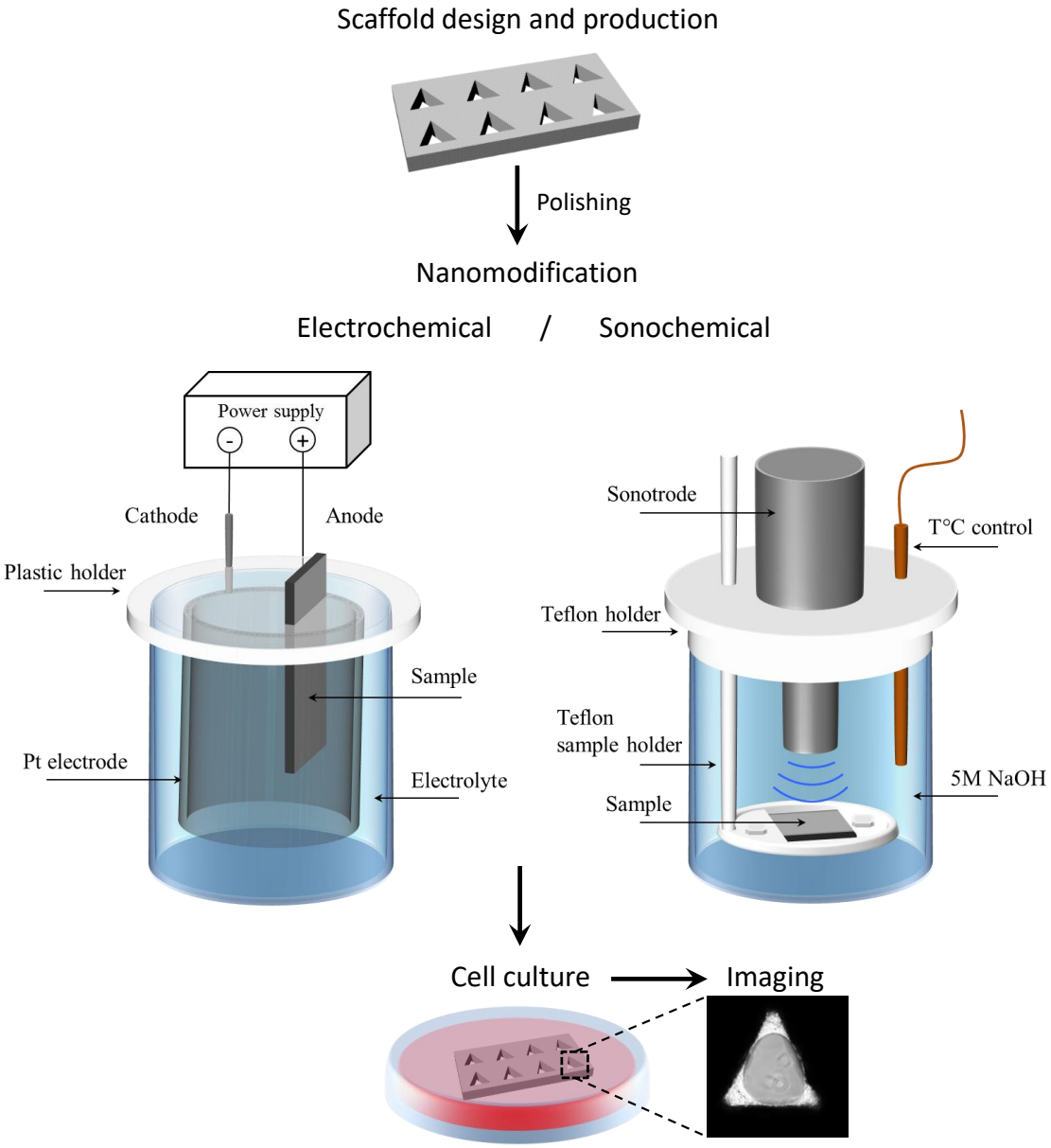

Figure 1. Experimental protocol. Scaffold fabrication by machining, followed by the application of the nanostructuring technique, either sonochemical treatment or anodic oxidation, to the scaffold. MC3T3-E1 Preosteoblasts are seeded (10^5 cells/cm^2) on the scaffolds and cultured for 7 days. Tissue growth is quantified by the phase contrast microscopy every day by measuring the projected tissue area (PTA) in each microchannel.

Atomic force microscopy (AFM)

Surface roughness measurements were performed using AFM in tapping mode. Analyses were conducted using micro cantilevers OMCL-AC160TS-W (Olympus, Japan) with a nominal resonance frequency of 300 kHz and a nominal spring constant of 42 N/m. Atomic force micrographs of a scan size 3 x 3 µm^2 were made on three different places on the sample under ambient atmosphere. Quantitative data about the values of surface roughness average (Img.

R_a) presented as mean over 3 measurements at different points on the surface, height profile, and three-dimensional projections of the micrographs were obtained using the software Nanoscope V614r1.

Contact angle measurements

Contact angle measurements were obtained using an optical tensiometer Krüss G23 M (Germany) equipped with a digital camera and image analysis software. Sessile drop contact angles of the air-water-substrate interface were measured three times over a period of 20 s on at least three samples of each surface nanomodification.

Cell culture model

A mouse calvarial preosteoblast cell line MC3T3-E1 was provided by the Ludwig Boltzmann Institute of Osteology, Vienna, Austria. Preosteoblasts were cultured for 5 – 7 days in α-MEM (Sigma-Aldrich, St. Louis, MO) supplemented with 10% (by volume) fetal calf serum (PAA laboratories, Linz, Austria), 4500 mg/L glucose, 0,1% (by volume) gentamycin (Sigma-Aldrich, Steinheim, Germany), 0,1% (by volume) ascorbic acid (Sigma-Aldrich, St. Louis, MO), and maintained at 37°C with 5% CO_2 in a humidified atmosphere. Cells were passaged in total three times every 48 hours by a dilution factor of 1/6. After reaching confluence, cells were dissociated from culture vessels by incubating with pronase for 3 – 5 min and seeded onto scaffolds at the density of 10^5 cells/cm^2. Scaffolds were autoclaved before cell culture experiments.

After 5 – 7 days, scaffolds were washed with phosphate buffer saline (PBS), fixed with 4% paraformaldehyde in PBS, and permeabilized with buffered Triton-X100 (Sigma-Aldrich, Steinheim, Germany) for 10 min at room temperature. Scaffolds were then thoroughly washed with PBS and stained for 60-90 min with phalloidin Alexa488 (Invitrogen, Oregon, USA) (1:20) in the dark at 4°C. After that scaffolds were thoroughly washed with PBS again, and stained for nuclei with TO-PRO3 iodide (Invitrogen, Oregon, USA) (1:300) for 5 min at room temperature. Scaffolds were washed with PBS, mounted with Fluoro-Mount (Southern Biotech) in inverted position on the glass slides, and examined via confocal microscopy (Leica Microsystems, Mannheim, Germany).

Microscopy and image acquisition

Each pore was imaged every 3 – 4 days using a phase contrast microscope (Nikon Eclipse TS100, Japan) equipped with a digital camera (Nikon Digital sight DS 2Mv). All pictures were

taken with a 10x objective, yielding the final image resolution 1 mm = 205 pxl. Imaging of the stained scaffolds was conducted by using a Leica confocal laser scanning microscope (Leica TCS SP5, Leica Microsystems, Mannheim, Germany). For doubly stained cells, phalloidin (actin stain) was excited with the argon laser line at 488 nm and TO-PRO3 (nucleus counterstain) with the He-Ne laser line at 633 nm. All images were captured with a PL FLUOTAR objective and collected in multichannel mode.

Tissue production in the pores was quantified as described in Bidan *et al*[24] using ImageJ 1.47 (NIH, USA). Phase contrast micrographs were binarised, and the contrast in the images enabled to distinguish the amount of tissue produced in the pores.

Statistical analysis

Data from experiments examining cell response are presented as mean ± standard deviation (SD) for three samples per each surface nanotopography. All experiments were repeated three times, and the results of the individual experiments are presented. Data were evaluated by one-way ANOVA, and the significance level of the groups' means was determined using Tukey test.

Results and discussion

Preparation and characterization of nanostructured 3D scaffolds

To study the impact of the first cell layer on 3D tissue growth, hexagonal 3D tissue engineering scaffolds (**Figure 2**A, B) each containing 8 channels with cross sections of different shapes (round, triangular, and square) of 500 µm side length/diameter and 1000 µm depth were cut from the 1 mm thick Ti plate. Perimeters and areas of the microchannels with different shapes are presented in **Table 1**. Sonochemical and electrochemical methods were applied to the scaffolds for the nanomodification of the Ti surface with the production of mesoporous and nanotubular titania surface layer, respectively.

Table 1. Perimeters (P, µm) and areas (A, μm^2) of the microchannels of different shape.

Microchannel shape	Perimeter, P [µm]	Surface area, A [μm^2]
Round	1570	108×10^3
Triangular	1500	196×10^3
Square	2000	250×10^3

Scanning electron microscopy of the original unmodified Ti surfaces revealed that they are relatively smooth at the nanoscale, with some submicroscale features caused either by machining for obtaining the microchannels or acid-etching (Figure 2C, G). In contrast, titanium surfaces that had received sonochemical or electrochemical treatment possessed homogeneous nanostructured surface layers (Figure 2D-I). Statistical image analysis (histograms are shown in Figure 2F, J) indicated that although the average pore diameters of the nanostructures on TMS and TNT were 65 and 75 nm, respectively, TMS had a broader pore size distribution than TNT. SEM images of the nanostructured scaffolds confirmed that in case of both treatments similar nanostructural features were generated both on external and internal surfaces, confirming the "non-line-of-sight" nature of these surface modification treatments.

Anodic oxidation was previously successfully used to generate well-defined highly ordered nanotubular titania topographies with diameters in the range of 60 – 11 nm and length of up to 650 nm on titanium mesh with complex geometry. [32] The titanium mesh consisted of about 100 µm-thick titanium wires and contained about 9 openings/mm^2. The nanotubes were grown in a radially outward direction around the titanium wire uniformly. The irregularities in nanotubular layer were observed only between the titanium wires at the joints of the mesh. For all chemical treatments, including anodic oxidation and sonochemical treatment, a direct contact of the electrolyte/working solution etc. with the metal surface is a necessary requirement for effective modification. [2] Therefore, if two surfaces are squeezed together, as two titanium wires in the mesh, the access of the electrolyte to the surface is limited, causing surface irregularities. Sonochemical treatment was not yet been shown for the modification of complex metal surfaces. However, it is a potentially industrially scalable process. For example, the upscaling of the process can be achieved by using special arrangements of multiple ultrasonic devices as was shown for the applications in food industry.[14] Moreover, manufacturers[15] of the ultrasonic devices offer a similar approach for the process upscaling in other applications, such as metal surface modification, by aligning multiple ultrasonic devices with respect to the area of the metal surface to be treated. In our study, sonochemical treatment was used to generate sponge-like mesoporous TiO_2 layer, covering the internal and external surfaces of the 3D titanium scaffolds. Thus, our observations support the general utility of the sonochemical treatment for the modification of titanium scaffolds with complex geometries, clinical and industrial applicability of this method.

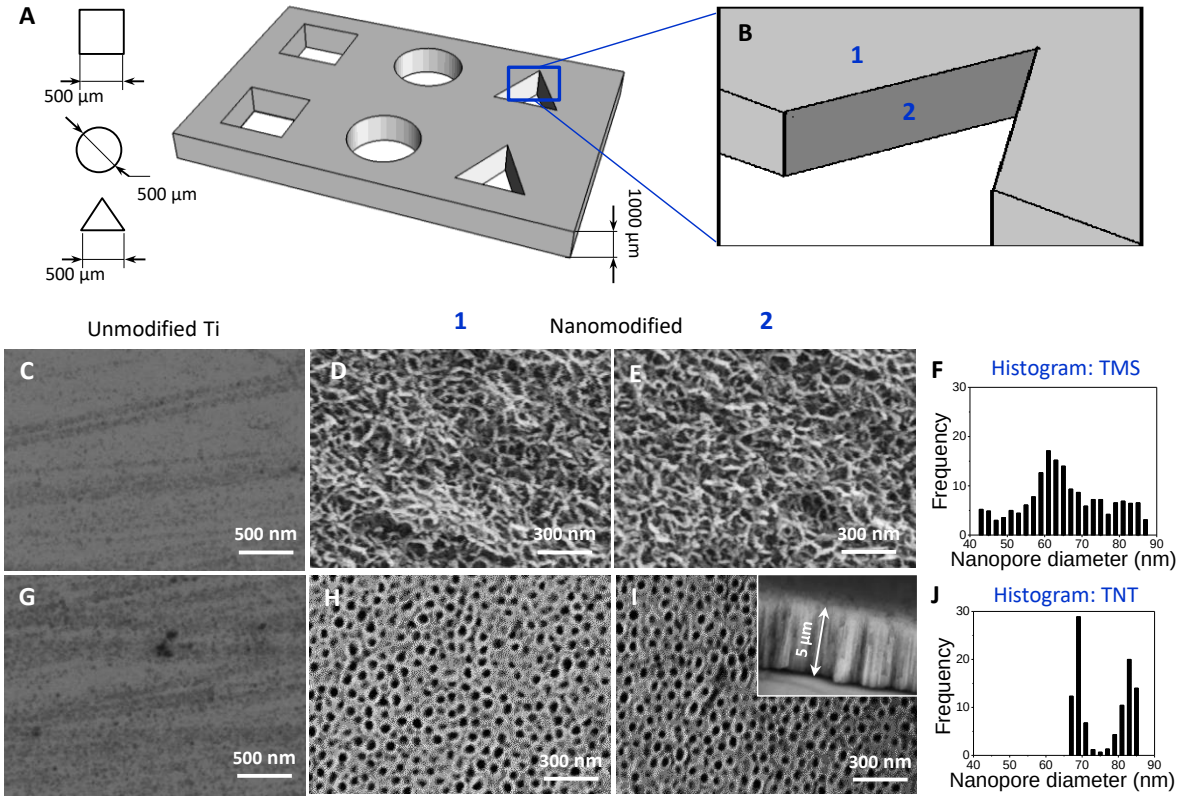

Figure 2. (A) Schematic structure of the 3D titanium scaffolds containing pores of different shape. (B) After cutting the scaffold along the pores, SEM investigation of the surface nanotopography outside (1) and inside (2) the pores could be performed. (C, G) High magnification images of the unmodified scaffold reveal that the surface was relatively smooth. Conversely, high magnification images of nanomodified implant surface display homogeneous coverage of nanostructures throughout exposed and non-line-of-sight areas. After the nanomodification with sono- and electrochemical treatments, (D, E) TMS and (H, I) TNT surfaces possessed relatively high and homogeneous coverages of nanostructures. (F, J) Image analysis of TMS and TNT surfaces revealed that the average nanopore diameter (when viewed from above by SEM) had very close values for both nanomodifications in the range of 65 – 75 nm, but with different pore size distributions.

Three-dimensional tissue growth

To investigate how surface nanotopography influences tissue formation at larger length scales than single cell layer, a series of experiments were performed in titanium scaffolds with 1000 µm deep pores (**Figure 3**).

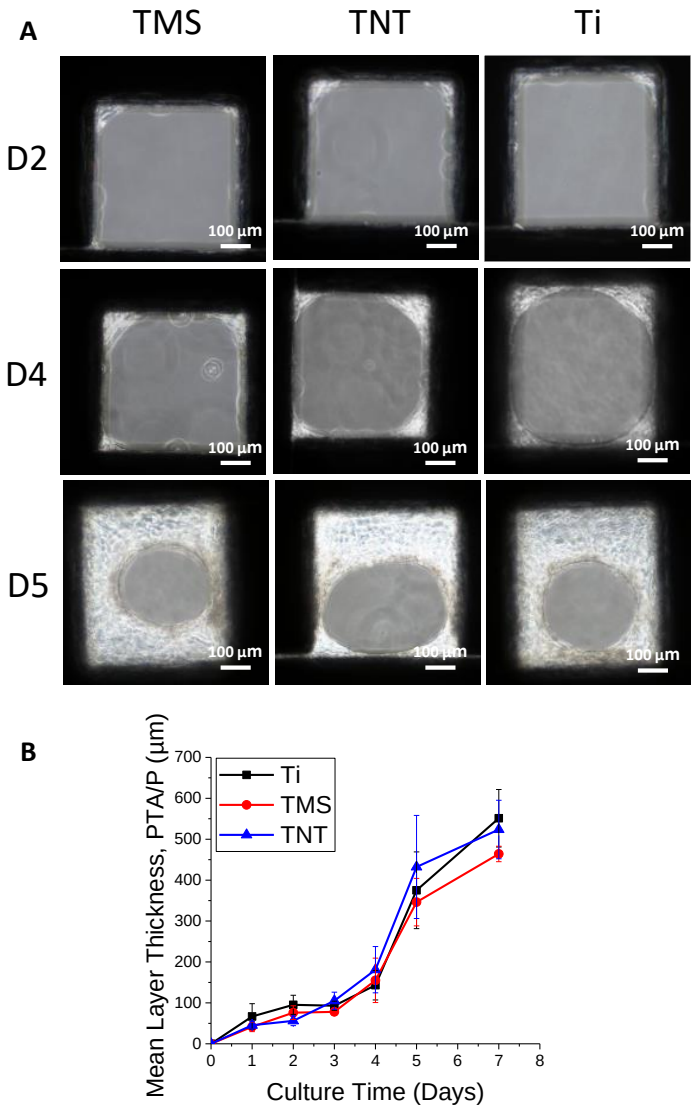

Figure 3. (A) Effect of surface nanotopography on MC3T3-E1 tissue growth in the microchannels of the square shape. Phase-contrast micrographs showing ingrowth of cell in pore channels of TMS, TNT and unmodified Ti scaffolds at different culture times of 2, 4, and 5 days. (B) Mean tissue layer thickness (calculated by the normalization of the projected tissue area, PTA to the perimeter, P) as a function of culture time. Data represent the mean value ± SD, n=9.

Quantitative data on tissue formation kinetics were obtained from three cell culture experiments over 7 days with nanomodified Ti 3D scaffolds containing 8 microchannels with three different cross-section shapes (round, triangular, and square). The mean thickness of the tissue layer (PTA/P)was estimated by measuring the projected tissue area (PTA) obtained from the phase contrast microscopy images of the microchannels (Figure 3A) taken over a period of 7 days, which was then normalized by the perimeter of the pore (P) to exclude the dependence on the pore area (Figure 3B). The comparison between the substrates did not

show significant differences between the growth rates verifying higher ones on TMS than on unmodified Ti scaffold and TNT.

In addition, with every additional cell layer, the tissue adhesion to the substrate seems to decrease. We observed the detachment of tissue from the microchannel walls of the nanostructured scaffolds, whereas the tissue on the unmodified Ti was not affected (**Figure 4**B). This process can be driven by (1) the increase of tension from the upper tissue layers transferred to the first layer, which is directly interacting with the substrate, and (2) by possible non-homogeneous cell density in some regions, causing misbalance in the distribution of tensile forces between single cells and cell layers and leading to detachment. Therefore, to further verify this misbalance and investigate the role of the first cell layer and its adhesion in 3D tissue formation, the scaffolds with partial nanostructuring were produced by masking ½ of the scaffold and leaving another ½ exposed to the nanostructuring treatment (Figure 4A). The goal of this investigation was to find how cells interact growing simultaneously on two different substrates. After 5 – 7 days, we observed tissue detachment from the TMS modified part (indicated by the arrows) and its rolling towards the unmodified part of the scaffold as shown in the fluorescent micrographs obtained with the Z-stack (Figure 4C). This phenomenon could be a consequence of the dominance of stress forces towards the unmodified part, caused by the stronger tissue adhesion on unmodified Ti than on nanostructured surface as shown in Chapter 3.

Multiple studies showed the impact of surface characteristics, such as topography, stiffness, and chemical composition, on cell and tissue growth both *in vitro* and *in vivo* (see Review[33]). However, little is known about the effect of nanotopography on 3D tissue growth. Microchannel-containing scaffolds were previously used to investigate an effect of surface geometry on bone like tissue growth.[27-29] The tissue growth kinetics in such systems were found to be independent of substrate stiffness, since further cell proliferation and differentiation occurs inside the cells own matrix.[34] In this study, to investigate the effect of surface nanotopography on 3D tissue growth, we performed a quantitative analysis of tissue growth rate within different microchannels of the 3D Ti scaffolds. The amount and the shape of the tissue produced by MC3T3-E1 preosteoblasts in the microchannels with nanostructured surfaces were quantified in term of PTA obtained from the phase contrast images taken over a period of 7 days.

As verified by confocal laser scanning microscopy, preosteoblasts were shown to proliferate and form a tissue-like network into the depth of the nanostructured Ti microchannels. Similar to the previous studies, the tissue growth behavior within the Ti microchannels followed the

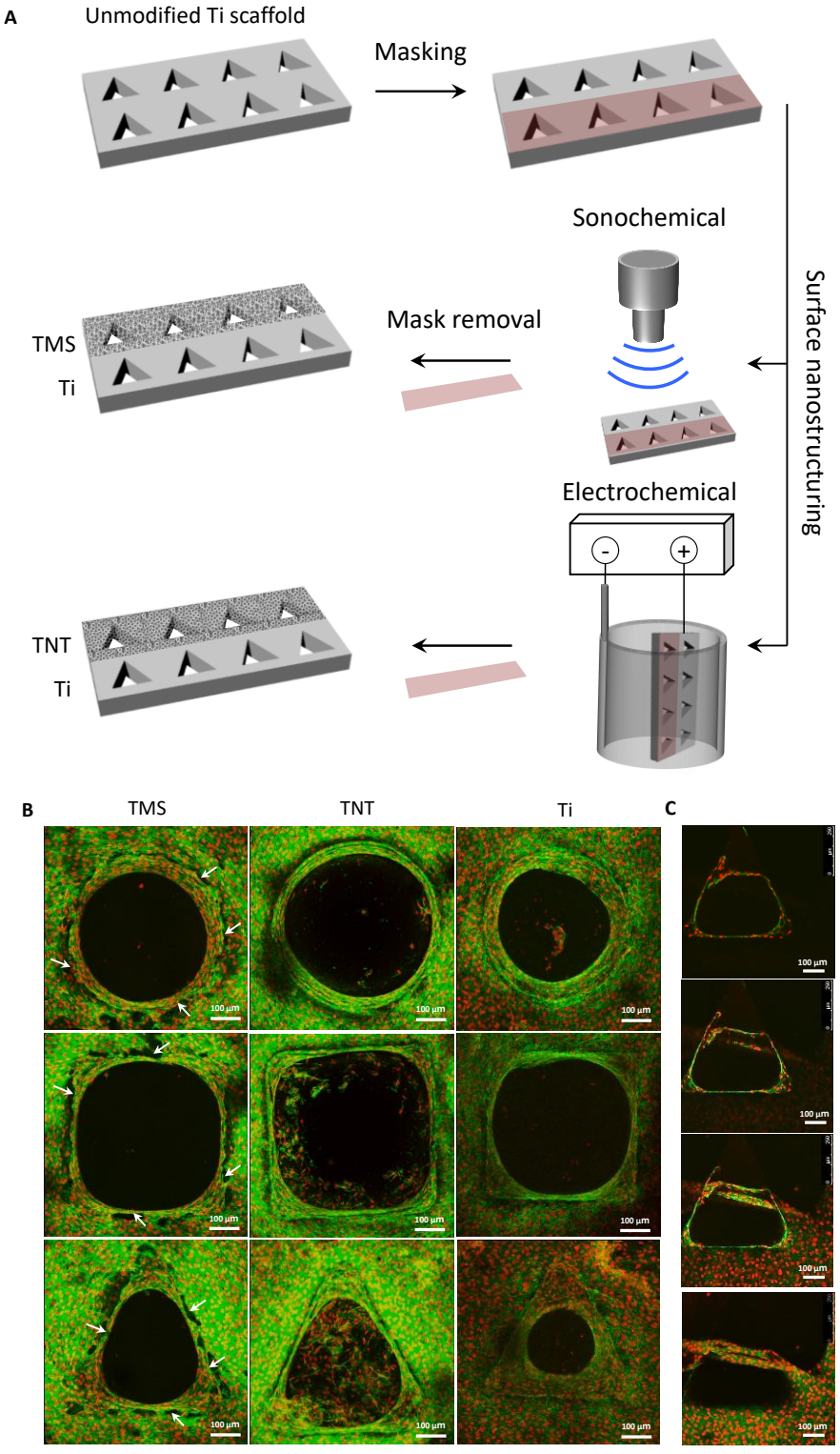

Figure 4. Tissue behavior in the microchannels with partial nanostructuring. (A) Schematic of partial nanostructuring of 3D tissue engineering scaffolds. (B) CLSM images with nuclear (red) and actin (green) staining showing bone tissue in the microchannels with TMS or TNT nanotopography inside and unmodified Ti. Tissue detachment is indicated with arrows. (C) Z-stack showing tissue detachment from the TMS modified part of the scaffold.

same steps as within the HA and PDMS scaffolds. First, the tissue formation started in the corners of the polygonal channels, whereas the tissue grew uniformly within the round channels. The differences in tissue thickness between the channels with different

nanostructuring were most pronounced in the corners of the triangular channels. Second, further tissue amplification led to the rounding of the corners and the formation of the round central opening. With further tissue growth, the opening was reducing with time by gradually becoming filled with tissue. In some cases, we observed the complete opening closure after 7 days of tissue growth. However, the opening closure was not due to the tissue amplification and its filling into the microchannels, but due to the tissue detachment and its displacement, causing the misleading observations. Moreover, similar to previous studies with MC3T3-E1 cells, the tissue formation rate on Ti scaffolds showed an initial linear growth phase.

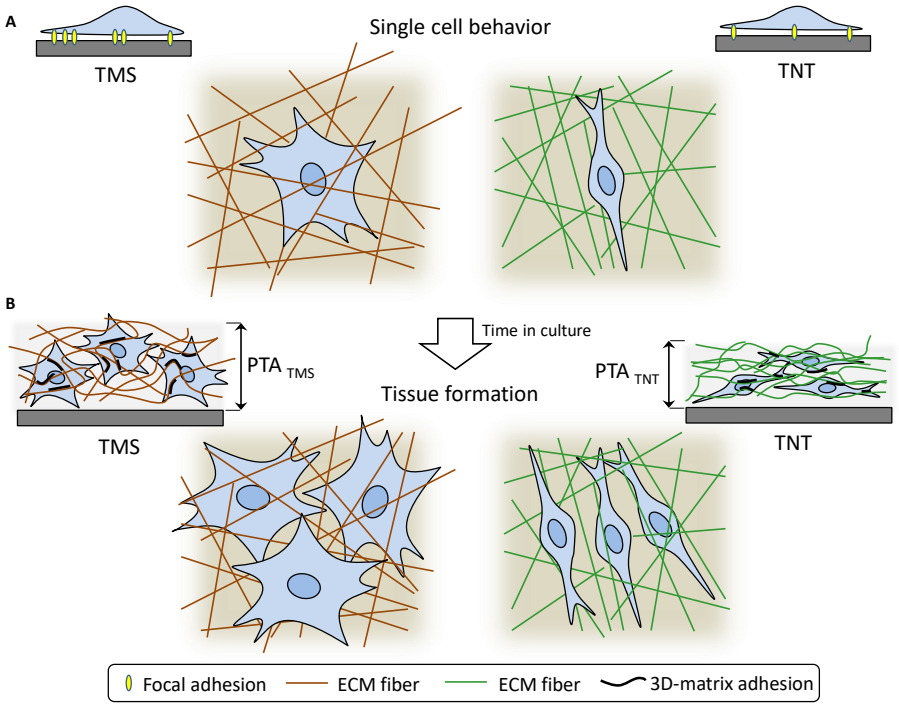

Figure 5. Schematic of tissue growth on TMS and TNT modified scaffolds based on the literature interpretation of the obtained results. (A) The titanium surface nanotopography affected single cell behavior and, in particular, cell proliferation, cell morphology (spreading, thickness), and cell adhesion. For example, the cells of the model cell culture were developing spreaded morphology with multidirectional protrusions and fibroblast-like morphology on TMS and TNT, respectively. Moreover, TNT strongly diminished cell adhesion as confirmed by the quantification of focal contact points. (B) The cell morphology and proliferation of the first cell layer may have an effect on the structure and the formation rate of the 3D tissue. The tissue formation rate is higher and the structure is denser on TMS than on TNT.

As shown in Chapter 3, the behavior of the first cell layer directly contacting the surface was affected by the nanotopography, in particular, proliferation, morphology, adhesion, and migration (**Figure 5A**). First, at the level of the single cell layer, cell proliferation on TNT was diminished compared to TMS and unmodified surface. Second, cells seeded on TMS displayed a spread morphology with multidirectional protrusions. In contrast, cells seeded on TNT displayed fibroblast-like morphology with unidirectional protrusions, indicating their migratory behavior. The effects of nanotopography on cell proliferation and cell morphology were still visible after 5 days of tissue growth (Figure 5B). Due to the lower number of cell nuclei and elongated morphology of cells on TNT, the tissue on TNT after 5 days displayed a loose structure with some surface still uncovered with cells. In contrast, the tissue on TMS and Ti displayed was denser with big number of cell nuclei and closer cell packing. Surprisingly, no significant differences between the surfaces were observed in tissue network formed in the corners, as indicated by the measurements of the mean tissue layer thickness.

Importantly, surface nanotopography affected cell adhesion. The number of focal contact points on both nanostructured surfaces was lower than on unmodified Ti, as indicated by the immunofluorescent staining of the first cell layer. Thus, cell adhesion on both nanostructured surfaces was diminished compared to the unmodified surface. This finding is however true only for the first cell layer, and it is challenging to quantify cell adhesion at later periods of tissue formation. Most of our current knowledge about cell adhesion is based on *in vitro* studies carried out with 2D cell cultures on unnaturally planar rigid substrates. The best-characterized adhesions formed by fibroblasts on 2D substrates are focal adhesions (FA) (also focal contacts) and fibrillar adhesions (FbA). In addition, Cukierman and co-workers[35-36] characterized the composition and function of so-called 3D-matrix adhesions (3D-MA), formed in 3D matrices derived from tissue or cell culture. 3D-MAs differ from focal and fibrillar adhesions formed on 2D substrates in the content of cytoskeletal components, biological activity and integrin usage. Due to their distinctive from classical 2D adhesions composition, localization and function, 3D-MA may be more biologically relevant. Based on these findings, Cukierman and co-workers proposed the cell adhesion maturation model illustrating the relationships and, most importantly, the evolution of cell-matrix adhesions *in vitro*. According to the proposed model, these three types of adhesions reflect different stages of interaction of cells with the ECM. Moreover, all types of matrix adhesions are related and appear in a specific consequence. Each type of adhesion is formed and disrupted in a dynamic, cyclical manner through sequential recruitment and loss of different integrin receptors, cytoskeletal and signalling molecules from the cytoplasm.

To date, the tissue maturation stages can be observed mainly by immunofluorescent labelling of different integrin-complex proteins involved in adhesion formation such as integrin and paxillin. This method indicates which type of cell adhesion is present at the particular stage of tissue growth, but it may not provide an adequate quantitative estimation of the strength of cell-substrate or cell-cell interactions within a tissue. Our approach to partially modify the 3D scaffolds allowed to investigate the effect of surface nanotopography on tissue behaviour. The observations of tissue detachment from the nanostructured surface and its rolling towards the unmodified part of the scaffold provided the strong evidence that the adhesion of the first cell layer could play a crucial role in 3D tissue formation.

Conclusion

In the present study, a simple and non-line-of-sight ultrasonic-based surface modification was highlighted for the superimposition of nanoscale structures on Ti scaffolds (as revealed by SEM and AFM analysis). In the proposed model, two surface nanotopographies with similar surface chemistry, but different order of nanotopography were examined – disordered HIUS-generated TMS and ordered TNT surfaces. These two nanostructured titania surfaces possess similar surface chemistry, but different nanotopography. In this study, the cellular responses of MC3T3-E1 preosteoblasts on the sono- and electrochemically nanomodified surfaces of titanium 3D tissue engineering scaffolds have been compared to evaluate how long nanotopography affects tissue growth. For this purpose, the growth kinetics of 3D tissue formation was investigated within the microchannels of the Ti scaffolds with different surface nanotopographies. Surprisingly, no significant differences in mean tissue layer thickness were observed between the surfaces. However, tissue detachment from the nanostructured scaffolds and its rolling towards the unmodified part of the scaffold in case of partially nanostructured scaffolds indicate the potential role of the nanotopography-modulated first cell layer in 3D tissue formation. These findings support the conclusion that the successful osseointegration of an implant-relevant material depends on the contribution from the first cell layer, especially, its adhesive behavior, and indicates its importance in 3D tissue growth.

Acknowledgement

We gratefully acknowledge Rona Pitschke and Heike Runge for performing SEM; Christine Pilz-Allen in assistance with cell culture; and Jan von Szada-Borryszkowski for fabrication of titanium scaffolds.

References

[1] F. Variola, J. Brunski, G. Orsini, P. T. de Oliveira, R. Wazen, A. Nanci, *Nanoscale* **2011**, *3*, 335.

[2] X. Liu, P. K. Chu, C. Ding, *Mater. Sci. Eng., R* **2004**, *47*, 49.

[3] A. M. Ballo, A. Palmquist, O. Omar, W. Xia, *Dental Implant Surfaces - Physicochemical Properties, Biological Performance, and Trends*, INTECH Open Access Publisher, 2011.

[4] A. L. Hook, N. H. Voelcker, H. Thissen, *Acta Biomater.* **2009**, *5*, 2350.

[5] F. Variola, F. Vetrone, L. Richert, P. Jedrzejowski, J.-H. Yi, S. Zalzal, S. Clair, A. Sarkissian, D. F. Perepichka, J. D. Wuest, F. Rosei, A. Nanci, *Small* **2009**, *5*, 996.

[6] C. Yao, T. J. Webster, *J. Nanosci. Nanotechnol.* **2006**, *6*, 2682.

[7] B. S. Necula, I. Apachitei, L. E. Fratila-Apachitei, E. J. van Langelaan, J. Duszczyk, *Appl. Surf. Sci.* **2013**, *273*, 310.

[8] S. Ferraris, A. Venturello, M. Miola, A. Cochis, L. Rimondini, S. Spriano, *Appl. Surf. Sci.* **2014**, *311*, 279.

[9] V. Dumas, A. Rattner, L. Vico, E. Audouard, J. C. Dumas, P. Naisson, P. Bertrand, *J. Biomed. Mater. Res., Part A* **2012**, *100A*, 3108.

[10] S. Amin Yavari, J. van der Stok, Y. C. Chai, R. Wauthle, Z. Tahmasebi Birgani, P. Habibovic, M. Mulier, J. Schrooten, H. Weinans, A. A. Zadpoor, *Biomaterials* **2014**, *35*, 6172.

[11] R. A. Gittens, T. McLachlan, R. Olivares-Navarrete, Y. Cai, S. Berner, R. Tannenbaum, Z. Schwartz, K. H. Sandhage, B. D. Boyan, *Biomaterials* **2011**, *32*, 3395.

[12] R. A. Gittens, R. Olivares-Navarrete, T. McLachlan, Y. Cai, S. L. Hyzy, J. M. Schneider, Z. Schwartz, K. H. Sandhage, B. D. Boyan, *Biomaterials* **2012**, *33*, 8986.

[13] Q. Y. Zeng, M. Xi, W. Xu, X. J. Li, *Mater. Corros.* **2013**, *64*, 1001.

[14] P. T. F. Swiergon, Juliana, P., Knoerzer, K., *2nd Meeting of the Asia-Oceania Sonochemical Society, Kuala Lumpur, Malaysia* **2015**, 41.

[15] https://www.hielscher.com/wire_01.htm.

[16] E. V. Skorb, D. G. Shchukin, H. Mohwald, D. V. Andreeva, *Nanoscale* **2010**, *2*, 722.

[17] E. V. Skorb, D. Fix, D. G. Shchukin, H. Mohwald, D. V. Sviridov, R. Mousa, N. Wanderka, J. Schaferhans, N. Pazos-Perez, A. Fery, D. V. Andreeva, *Nanoscale* **2011**, *3*, 985.

[18] Y. Zhukova, S. A. Ulasevich, J. W. C. Dunlop, P. Fratzl, H. Möhwald, E. V. Skorb, *Ultrason. Sonochem.*, http://dx.doi.org/10.1016/j.ultsonch.2016.11.014.

[19] J. M. Macak, H. Tsuchiya, A. Ghicov, K. Yasuda, R. Hahn, S. Bauer, P. Schmuki, *Curr. Opin. Solid State Mater. Sci.* **2007**, *11*, 3.

[20] A. Ghicov, P. Schmuki, *Chem. Commun.* **2009**, 10.1039/b822726h, 2791.

[21] M. J. Dalby, N. Gadegaard, R. O. C. Oreffo, *Nat. Mater.* **2014**, *13*, 558.

[22] D. Karazisis, A. M. Ballo, S. Petronis, H. Agheli, L. Emanuelsson, P. Thomsen, O. Omar, *Int. J. Nanomed.* **2016**, *11*, 1367.

[23] K. C. Popat, L. Leoni, C. A. Grimes, T. A. Desai, *Biomaterials* **2007**, *28*, 3188.

[24] F. Pampaloni, E. G. Reynaud, E. H. K. Stelzer, *Nat. Rev. Mol. Cell Biol.* **2007**, *8*, 839.

[25] E. Tamjid, A. Simchi, J. W. C. Dunlop, P. Fratzl, R. Bagheri, M. Vossoughi, *J. Biomed. Mat. Res. A*, **2013**, *101A*, 2796.

[26] S. Janbaz, R. Hedayati , A. A. Zadpoor, *Mater. Horiz.,* **2016**, 3, 536.

[27] M. Rumpler, A. Woesz, J. W. C. Dunlop, J. T. van Dongen, P. Fratzl, *Journal of The Royal Society Interface* **2008**, *5*, 1173.

[28] C. M. Bidan, K. P. Kommareddy, M. Rumpler, P. Kollmannsberger, P. Fratzl, J. W. C. Dunlop, *Adv. Healthcare Mater.* **2013**, *2*, 186.

[29] C. M. Bidan, K. P. Kommareddy, M. Rumpler, P. Kollmannsberger, Y. J. M. Bréchet, P. Fratzl, J. W. C. Dunlop, *PLoS ONE* **2012**, *7*, e36336.

[30] L. D. Quarles, D. A. Yohay, L. W. Lever, R. Caton, R. J. Wenstrup, *Journal of Bone and Mineral Research* **1992**, *7*, 683.

[31] M. Rumpler, A. Woesz, F. Varga, I. Manjubala, K. Klaushofer, P. Fratzl, *Journal of Biomedical Materials Research Part A* **2007**, *81A*, 40.

[32] Q.-Y. Zeng, M. Xi, W. Xu, X.-J. Li., *Materials and Corrosion* **2013**, *64*, 1001.

[33] C. J. Bettinger, R. Langer, J. T. Borenstein, *Angew. Chem. Int. Ed. Engl*. **2009**, *48*, 5406.

[34] K. P. Kommareddy, C. Lange, M. Rumpler, J. W. Dunlop, I. Manjubala, J. Cui, K. Kratz, A. Lendlein, P. Fratzl, *Biointerphases* **2010**, *5*, 45.

[35] E. Cukierman, R. Pankov, D. R. Stevens, K. M. Yamada, *Science* **2001**, *294*, 1708.

[36] E. Cukierman, R. Pankov, K. M. Yamada, *Curr. Opin. Cell Biol.* **2002**, *14*, 633.

Chapter 4: Supporting information

Chapter 4. How Important Is the First Cell Layer for Tissue Organization: Surface Nanostructuring and Tissue Growth in 3D Titanium Microchannels?

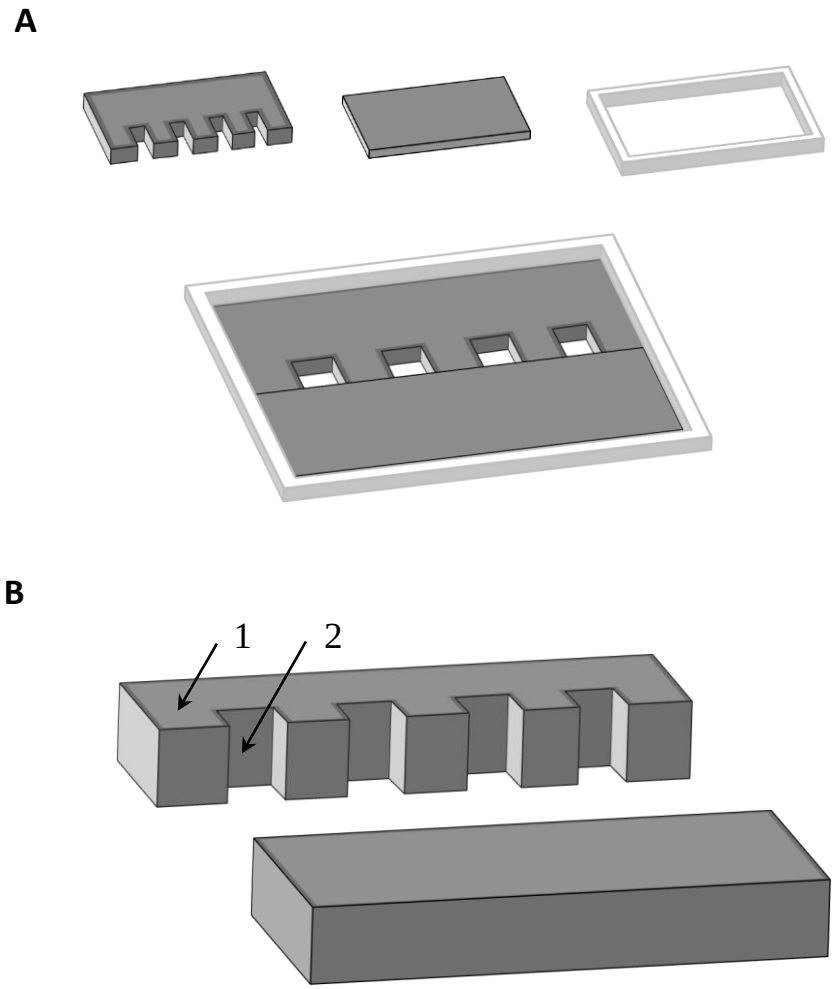

Figure S1. Example of a 3D tissue engineering scaffold design developed to confirm the "non-line-of-sight" nature of the nanomodifications strategies. (A) Scaffold consists of two Ti parts with one part having 500 µm-sized square openings and a Teflon frame holding two parts together during the nanomodification treatment (sono- or electrochemical). (B) Surfaces of interest are depicted with arrows 1 and 2, pointing at the external plain surface of the scaffold and at the internal walls of the microchannnel, respectively. SEM measurements are performed at these regions.

Chapter 5. General discussion

The main goal of this thesis was to understand how surface nanotopography modulates cell and tissue behaviour. Chapters 1 – 4 present the key findings of this research question in the form of four first-author publications. Two additional publications are given in the Appendices.

Back to the objectives

First, the scope of this thesis was introduced by the literature review (Chapter 1) highlighting the methods for titanium surface nanostructuring. In particular, this review chapter highlighted electrochemical and sonochemical methods for nanostructuring, as well as the known effects of titanium surface nanotopography on cell behaviour.

Next, the straight-forward method of sonochemical formation of mesoporous titania surface (TMS) under HIUS treatment in alkaline solution was presented in detail (Chapter 2). The main results of this study are the following:

- Short (5 – 15 min) HIUS treatment in alkali conditions has induced the formation of a sponge-like titanium dioxide surface layer. This layer possesses nanoscale surface roughness and is highly hydrophilic as verified by AFM and contact angle measurements, espectively.

- The formation of the interpenetrating nanostructured titanium dioxide layer on bulk Ti, verified by HRTEM, indicates its strong integration with a bulk metal. This is the first indication that the sonochemical treatment can be potentially applied for large-scale surface modification.

- Good cytocompatibility of TMS was confirmed using the MC3T3-E1 preosteoblast cell line.

Due to its unique nanotopography, physicochemical properties and biocompatibility, sonogenerated mesoporous titania (TMS) is a potential candidate for biological applications. In comparison to well-studied nanotubular titania (TNT) and a glass control, mesoporous titania was used to investigate the cell-nanotopography interactions at the early stages of tissue growth as shown with a MC3T3-T1 preosteoblast cell culture model (Chapter 3). The main results of this study are the following:

- Cell proliferation on TNT was diminished in comparison to TMS and the glass control.
- Cells on TMS and glass control developed spread morphology with multidirectional protrusions. In contrast, cells on TNT developed fibroblast-like norphology with unidirectional protrusions.
- Cells exhibited lower number of focal contact points on both nanostructured surfaces than on glass control. However, the co-localization analysis of focal contact points indicates the formation of the stable mature adhesions on TMS and unstable nascent adhesions on TNT.
- The highest cell migration speed was observed on TNT, which is in good agreement with observations of migratory polarized cell morphology and formation of unstable nascent adhesion points exhibited by cells on TNT.

The distinct nanotopography-modulated cell behaviours indicated a role of nanotopography in early tissue formation, leading to the next study, making the step towards understanding of the cell-nanotopography interactions in 3D tissue (Chapter 4). The main results of this study are the following:

- The 3D scaffolds treated either sonochemically or electrochemically possessed identical nanostructural features on both external and internal surfaces as verified by SEM. This observation confirms the “none-line-of-sight” nature of these surface treatments and their potential to large-scale surface modification.
- The thickness of the tissue layer formed after 7 days of growth did not show significant differences between the surfaces.
- On partially modified 3D scaffolds, tissue detachment and its rolling towards the unmodified part of the scaffold were observed, indicating poor adhesion to the nanostructured Ti surface.

Thus, the results suggest the potential of the surface treatments discussed in this thesis, in particular of sonochemical treatment, for the modulation of cell behaviour and the potential application of these methods for larger-scale surface modification. However, further studies deeper investigating molecular mechanisms and HIUS effects should be performed.

Implications of the study

In the studies shown in this thesis, we looked at the modified Ti surfaces with uniform nanofeatures. However, there would also be interest in producing and investigating surfaces with non-uniform nanofeatures. One reason to introduce surface nanopatterning would be to produce gradients in structure that mimick closely those seen in Nature (see Review [26]). To achieve this future work is required to develop the HIUS technique to allow for the formation of metal surfaces with multihierarchical patterned topographies. Such surface patterning could be performed either by tilting of the metal surface under the sonotrode or by surface masking. In addition to allowing controlled patterning/nanostructuring. Such control of the HIUS technique would also be useful in gaining a deeper understanding of the sonochemical methodology for metal modification.

The potential for micropatterning of the Ti surface using HIUS has already been demonstrated recently by surface masking.[27] The initial aim of these studies was to gain knowledge of cavitation process at the solid surface in the HIUS treatment. Firstly, a model of heterogeneous nucleation of cavitation bubbles was formulated.[28] By changing the surface energy (initial wettability of the patterned surface) it is possible to achieve a selective control of the heterogeneous nucleation of gas bubbles near the solid-water interface. Higher contact angles cause a lower energy barrier, and therefore cavitation effect and surface nanostructuring are more pronounced at hydrophobic surfaces.[29-30] These works are of great interest for biological and biomedical applications. They provide not only a significant contribution to the investigation of acoustic erosion on metals, but also propose new application of HIUS treatment for the production of patterned metal surfaces with defined physical or chemical properties. However, it is still not clear whether surface tilting during sonication could play a role in the resulting surface topography. In the theory of acoustic cavitation, different factors can affect cavitation bubble behaviour such as effects of gas and particulate matter, viscosity, applied frequency, and temperature.[31] The distance from the sonotrode may also affect the final surface properties[32], which may be able to be used to create novel surface nanostructuring.

For example, formation of structural gradients with nanopore topography using angled arrangement of the surface during the electrochemical anodization has been shown by Kant *et al.*[33] It is well-known that the diameters of anodic aluminum oxide (AAO) pores formed during anodization can be controlled by various factors[34] such as voltage [35] and by inter-electrode spacing[36]. A distinct anodization condition with an asymmetrically distributed electric field was created due to the angular arrangement between the electrodes in order to achieve gradual distribution of the current density and temperature. Structural, optical and wetting gradients on aluminum were prepared in this manner. Characteristic brushlike structures were observed at the point closest to the cathode. As the distance between the electrodes

increased, the gradual decrease of brush length was observed till the formation of a very short nanotip structure. Moreover, the biological study[33] has demonstrated that pore organization has an influence on the orientation, morphology and attachment of neuronal cells. The most extensive cell response was found on the surfaces with mixed pore and brush structure, where the cells exhibited some neuritelike phenotype with cytoplasmic processes and the most extensive cell-cell interactions. Cells cultured on pores without brushes and tips structures had a more neuritelike phenotype with long bipolar cytoplasmic processes, similar to the axon and dendrite emerging from opposite ends of a neuronal cell. These cells had their neuritelike processes that aligned with the direction of the pore structures.

In Chapters 2 and 4, we investigated a potential application of the sonochemical treatment for larger-scale surface modification of Ti. We have shown (1) formation of the interpenetrating nanostructured titanium dioxide layer on bulk Ti, verified by HRTEM, indicating its strong integration with a bulk metal; (2) formation of the identical surface nanofeatures on the external and internal surfaces of the 3D scaffolds, verified by SEM, indicating the “non-line-of-sight” nature of the sonochemical treatment. However, how complex the geometry of the scaffold can be to be modified effectively still remains unclear. Further scaffold geometries with various shapes and dimensions should be thoroughly examined in future work to find the spatial limits of the modification method.

The amount of the tissue formed in the 3D scaffolds did not show a significant difference between the surfaces. However, differences in tissue structure have been verified by the actin staining. Dense tissue was observed on TMS and Ti scaffolds, whereas loose tissue with not complete covering of the scaffold was observed on TNT. We suggest that these differences in 3D tissue could have a connection to the observations of the early-stage cell behaviour made in Chapter 3. For example, due to diminished cell proliferation and fibroblast-like morphology of cells on TNT, complete surface coverage was not achieved on this surface even after 5 days of growth. Moreover, we observed tissue detachment from the nanostructured surfaces, also its rolling towards the unmodified part of the scaffold with partial nanostructuring, suggesting poor adhesion on nanostructured surfaces. The results provided in Chapter 3 indicated that each surface, TMS and TNT, induced specific cell adhesion. As verified by the amount of focal contact points and their colocalization with F-actin, cells on TMS tend to develop stable mature adhesions, whereas cells on TNT develop nascent unstable adhesions. This observation goes in line with the polarized cell morphology and high migration speed on TNT indicating cells migratory behaviour on TNT. To study cell adhesion in Chapter 3, we performed immunofluorescent staining for vinculin as one of the best studied integrin-complex proteins widely used for labelling cell adhesion (see Review [37], [38]). However, this information is not

enough to make conclusions on the adhesion maturation stages, which cells develop on Ti surfaces, and more studies investigating adhesions turnover are required. One of the most informative approaches to study adhesion turnover would be to set-up a time-lapse analysis/life cell imaging[39] to follow focal adhesion persistence over time as was previously shown in the similar studies with Ti surfaces.[40-41] Fluorescently labelled markers such as paxillin should be used for the determination of early adhesion; zyxin, p130Cas, etc. – of late adhesion (see Reviews [42-43]).

Thus, we already have some indication of poor adhesion in 3D system, but further investigation of molecular mechanisms and their interplay within 2D and 3D systems is necessary. It is likely that the dimensionality of the matrix contributes to adhesion organization. The relative cellular distribution of the different types of adhesions is dependent on the composition and mechanical properties of the ECM (see Review [42]). The size of adhesions in cells in 3D matrices resembles those formed by cells on more pliable soft substrates, having smaller and more dynamic adhesions. The adhesions of cells attached to large collagen fibres are large and oriented along the fibres in a 2D-like organization.[44]Therefore, to understand the poor adhesion in the 3D system described in Chapter 4, we propose two further studies: (1) investigation of the ECM composition/dimensionality/fibre orientation by (immuno)fluorescent staining for the ECM proteins such as fibronectin, vitronectin, laminin and various collagens;[38] and (2) investigation of the viscoelastic properties of the ECM by means of AFM force spectroscopy. To visualize the supramolecular assembly of collagen structure, second-harmonic generation (SHG) microscopy can be used as a new powerful tool.[45] AFM is also a powerful tool, which can be used not only due its high-resolution imaging capabilities but also for sensitive force measurements.[46] It can be used to study cell-substrate and cell-cell interactions by measuring the mechanical forces generated in the 3D system. Several processes such as adhesion, force generation by moving cells and dynamic reorganization of the cytoskeleton can be observed by AFM force spectroscopy.

To conclude, the data presented in this thesis contribute to the current body of literature on mechano-chemical interactions taking place at the cell-surface interface within 2D and 3D systems. However, much more remains to be learned about the dynamics of molecular mechanisms and signaling at cell adhesion sites on different surfaces. Therefore, we propose at least four more directions for further research: (1) development of surface nanopatterning strategies with sonochemical treatment by means of angular arrangement of the surface within the experimental setup; (2) determination of the limiting geometrical features (shapes, dimentions) for 3D scaffold modification with sono-and electrochemical treatments; (3) investigation of adhesions turnover by means of time-lapse imaging of the fluorescently

labelled early- and late-adhesion markers; (4) investigation of the ECM composition and its viscoelastic properties by means of SHG and AFM, respectively.

Conclusions and perspectives

The present thesis focuses on the understanding how the surface nanotopography affects cell and tissue growth. Surface nanostructuring has a great potential for biotechnological and biomedical applications such as anticorrosive and antibacterial surfaces, encapsulation, and modulation of cell behavior. The literature review of the topic provided the background motivation of the present thesis (Chapter 1). The enthusiasm for surface modifications arises from their versatility, physicochemical properties of the produced surfaces, their biocompatibility, and large specific surface area. However, the majority of the nanostructuring methods have some major limitations, since they cannot be applied for large-scale manufacturing, in particular, for nanostructuring of commercial or other implant-relevant scaffolds/devices of complex geometries. Therefore, this thesis presents a new platform for titanium surface nanostructuring, which allows for effective scalable modification of Ti surface and production of porous titania surfaces suitable for biological applications.

For this purpose, mesoporous titania surfaces (TMS) have been fabricated by a method based on high-intensity ultrasound (HIUS) treatment in presence of alkali solution (Chapter 2). This work has contributed to the fundamental understanding of the mechanism of acoustic cavitation at the titanium surface in combination with alkali treatment. This method allowed for a precise control over physical, chemical, and structural properties of the titanium surface by controlling the treatment parameters such as ultrasound intensity and duration of treatment. Sonication in alkali conditions has induced changes of surface nanotopography, wettability, and crystallinity of the titania surfaces. Short (5 – 15 min) HIUS treatment was sufficient for formation of a nanostructured titanium dioxide surface with high porosity and wettability as verified by AFM and contact angle measurements, respectively. Moreover, the formation of the interpenetrating nanostructured oxide layer on bulk Ti was verified by HRTEM, thereby indicating its high bonding strength and firm integration with a bulk metal and, therefore, the potential suitability of this method for large-scale surface modification. Furthermore, cell culture studies using the MC3T3-E1 preosteoblast cell line confirmed good cytocompatibility of TMS surface, thereby indicating its potential for biological applications.

The potential of the TMS surfaces was then tested in two studies, aiming to investigate the effect of surface nanotopography on single cell behavior (Chapter 3) and 3D tissue formation (Chapter 4).

To investigate the effect of surface nanotopography on single cell behaviour (Chapter 3), two titania nanotopographies have been used: mesoporous titania (TMS) and nanotubular titania (TNT). TMS and TNT were fabricated by the novel sonochemical method, presented in Chapter 2, and by the well-studied electrochemical method, respectively. These two surfaces possess distinct nanotopographical features of titania, but similar surface chemistry: (1) disordered sponge-like nanotopography of TMS and ordered nanotubular titania of TNT was detected by SEM; (2) the surface roughness at the nano-scale was in the range of 20 – 35 nm for both surface modifications as verified by AFM; (3) both surfaces are highly hydrophilic (contact angle below 15°) as detected by contact angle measurements. Next, the MC3T3-E1 preosteoblast response (proliferation, morphology, adhesion, and migration) to these surface nanotopographies has been investigated. First, cell proliferation was affected by nanotopography, i.e. TNT diminished proliferation in comparison to TMS and the control glass surface. Second, cell morphology was affected by nanotopography: cells exhibited a spread morphology with multidirectional protrusions on TMS and fibroblast-like morphology with unidirectional protrusions on TNT. Third, immunofluorescent staining against vinculin verified a diminished cell adhesion on both nanostructured surfaces in comparison to the glass control. Finally, a quantitative wound healing assay in combination with live-cell imaging allowed to estimate the migratory behaviour of cells on surfaces. The analysis of the mean migration speed and the mean amount of neighbouring cells confirmed that the cell migration on TMS has a more collective character than on TNT and control. Thus, the findings of this study indicated distinctly different cell adhesion and migration on ordered and disordered titania nanotopographies, providing important information that could be used in optimizing titanium-based scaffold design.

Next, the role of surface nanostructuring in 3D tissue formation was investigated (Chapter 4). For this purpose, the 3D scaffolds with microchannels of different shape and size, previously designed for investigation of the curvature-controlled 3D tissue growth,[22-25, 53] were fabricated out of bulk Ti and were modified by the two nanostructuring methods (sono- and electrochemical). First, SEM has showed that in case of both treatments both external and internal surfaces of the scaffold possessed similar nanostructural features, thereby confirming the “none-line-of-sight” nature of these surface treatments and their potential to larger-scale surface modification. Second, the rates of 3D tissue growth in the microchannels have showed only mild differences between the surfaces. However, the tissue grown on TMS has shown the detachment and, additionally, on surfaces with partial nanostructuring rolling towards the unmodified part of the scaffolds. Such tissue behaviour was not detected on unmodified

scaffolds, suggesting that the diminished adhesion of the first cell layer may have caused the observed tissue detachment after 7 days of growth. Moreover, the tissue structure was different on the surfaces: due to diminished proliferation and cells fibroblast-like morphology on TNT, the 3D tissue exhibited loose structure and was not reaching the complete coverage. Thus, the results suggested that the tissue formation rate, structure, and detachment of the tissue formed in the microchannels of the scaffolds could be affected by surface nanotopography, indicating important implications towards the understanding of the effect of nanotopography on tissue formation as well as towards the scaffold design for improved implant osseintegration *in vivo*.

To summarize, the titania surfaces presented in this thesis modulated the *in vitro* cell response and 3D tissue formation. Their performance was due to their distinct physicochemical and biological properties, such as biocompatibility, nanotopography, porosity, hydrophilicity, etc. Therefore, these nanostructured surfaces show potential for a wide range of biotechnological and biomedical applications. Moreover, due to photocatalytic properties of titanium dioxide,[54] nanostructured surfaces can be employed for the development of smart stimuli-responsive systems for modulation of cell behaviour. For example, the system containing the TMS surfaces presented in this thesis and a pH-responsive LbL coating has been recently shown to guide cell migration.[55] Further work is on-going on the development of “intelligent” titania-based hybrid polymer systems for biological applications as well as on further understanding of the mechanisms of the nanotopography-modulated cell adhesion.

Publications

1. Zhukova, Y.; Skorb, E. V.
   Cell Guidance on Nanostructured Metal Based Surfaces
   Advanced Healthcare Materials **2017**, 1600914.

2. Zhukova, Y.; Ulasevich S. A.; Dunlop, J. W. C.; Fratzl, P.; Möhwald, H.; Skorb, E. V.
   Ultrasound-Driven Titanium Modification with Formation of Titania Based Nanofoam Surfaces
   Ultrasonics Sonochemistry **2017***,* 36, 146 – 154.

3. Zhukova, Y.; Hiepen, C.; Knaus, P.; Osterland, M.; Prohaska, S.; Dunlop, J. W. C.; Fratzl, P.; Skorb, E. V.
   The Role of Titanium Surface Nanotopography on Preosteoblast Morphology, Adhesion and Migration
   Advanced Healthcare Materials **2017**, accepted.

4. Zhukova, Y.; Baidukova, O.; Dunlop, J. W. C.; Fratzl, P.; Skorb E. V.
   Patterned sonochemical treatment of 3D titanium scaffold with microchannels for testing the role of the first cell layer for tissue organization
   Manuscript in preparation.

5. Kopf, J.; Ulasevich, S.; Baidukova, O.; Zhukova, Y.; Dunlop, J. W. C.; Fratzl, P.; Rikeit, P.; Knaus, P.; Poznyak, S. K.; Andreeva, D. V.; Skorb, E. V.
   Ultrasonically Produced Porous Sponge Layer on Titanium to Guide Cell Behavior
   Advanced Engineering Materials **2016**, 18(4), 476 – 483.

6. Ulasevich, S. A.; Brezhneva, N.; Zhukova, Y.; Möhwald, H.; Fratzl, P.; Schacher, F. H.; Sviridov, D. V.; Andreeva, D. V.; Skorb, E. V.
   Switching the Stiffness of Polyelectrolyte Assembly by Light to Control Behavior of Supported Cells
   Macromolecular Bioscience **2016**, 16(10), 1422 – 1431.

Appendices

Appendix 1. Ultrasonically produced porous sponge layer on titanium to guide cell behavior

Jessica Kopf,[2] Svetlana Ulasevich,[1] Olga Baidukova,[1] Yulia Zhukova,[1] John W. C. Dunlop,[1] Peter Fratzl,[1] Paul Rikeit,[2] Petra Knaus,[2] Sergey K. Poznyak,[3] Daria V. Andreeva,[4] Ekaterina V. Skorb*[1]

[1] Max Planck Institute of Colloids and Interfaces, 14424 Potsdam, Germany

[2] Institute for Chemistry/Biochemistry, Freie Universität Berlin, 14195 Berlin, Germany

[3]Institute for Physico-Chemical Problems, Belarusian State University, 220030 Minsk, Belarus

[4] Physical Chemistry II, Bayreuth University, 95440 Bayreuth, Germany

* Corresponding author

Standard set statement from the publisher:
"This is the accepted version of the following article: [Kopf, J., Ulasevich, S., Baidukova, O., Zhukova, Y., Dunlop, W. C. J., Fratzl, P., Rikeit, P., Knaus, P., Poznyak, S. K., Andreeva, D. V., Skorb, E. V. (2016), Ultrasonically Produced Porous Sponge Layer on Titanium to Guide Cell Behavior. Adv. Eng. Mat., 18(4): 639-647. doi:10.1002/adem.201500456], which has been published in final form at [http://dx.doi.org/10.1002/adem.201500456]."

My Contribution: I performed titanium surface nanostructuring and discussion of cell culture experiments.

The adhesion of cells to surfaces, as well as their proliferation, migration, and differentiation, is guided not only by chemical functionalization but also by surface nanostructuring, nanotopography.[1] Nano-patterned titanium surfaces are one example in which the scale of patterning controls the size of focal adhesions.[2] Nanoscale disorder in surface structure can be used to stimulate cell differentiation[3] or can also be used to maintain stem cell phenotypes over long times.[4] Nanoroughness modulates cells interactions and function via mechanosensing.[5] These all suggest that the careful control of surface nanostructure of such important as titanium (Ti) biomaterial[6] could be a useful tool to achieve desired cellular responses.

We first time highlight that ultrasonic treatment is able to produce surface porous sponge layer in Ti. We find it great technological advances that Ti can be also modified with high-

intensity ultrasonic treatment. We really think that presenting high-intensity ultrasonic technique for Ti nanostructuring increases interest of scientists to the technique. Great advantage of our methodology is a large number of synthetic parameters which can be optimized to tune surface nanostructuring in a controllable manner. Moreover, this methodology will be very interesting in future to provide single-step hybrids and effective loading of porous structures with active chemicals. We compare our methodology with more known for bio-application anodization for surface nanostructuring.

Anodization leads to TiO_2 nanotube arrays covering the surface of titanium and is one of the most studied methods to develop porous surface nanotopographies with controlled pore sizes.[6] It has been demonstrated in cell culture experiments on TiO_2 nanotube arrays of different sizes that adhesion, proliferation, and migration of mesenchymal stem cells are optimal on ordered nano-pore arrays with spacings in the range of 15–30 nm; these length scales also lead to significantly less apoptosis than on 100 nm structures.[7, 8] It should be taken into account that nanostructuring does affect cell function at many levels but in a cell specific manner, and smaller surface features (50 nm) tend to favor cell proliferation in comparison to larger features (300 nm).[9]

Anodization requires a conductive substrate, is difficult to use over large surface areas, and uses aggressive media for synthesis.[6] Recently, we have shown that ultrasonic treatments in aqueous media can produce surface porosities in various size-ranges also below 100 nm in metals such as Al or Mg.[10] Here, we demonstrate that such nanostructuring can also be effectively induced in an important biomaterial, titanium, by investigating its influence on cell behavior in comparison to the well-established electrochemical method.

To this end, we investigate the response in terms of morphology, adhesion, proliferation, and differentiation of C2C12 cells on a glass substrate and on three different titanium/TiO_2 surfaces: a titania mesoporous sponge layer (TMS) formed by ultrasonication, a titania nanotube layer (TNT) with comparable porosity formed by anodization, and an unmodified titanium surface (Ti) covered with a flat native oxide layer (**Figure 1)**.

We focus on medium porosity (40–70 nm) nanostructures, which can be potentially used for surface drug delivery[11] while still allowing for cell adhesion and survival. It is seen from histogram, Figure 1, that the average pore size analyzed for TNT and TMS is the same, ca. 70 nm, however, for ordered TNT it is narrow pore size distribution and for disordered TMS the pore size distribution is broader to TNT. The critical value for TNT surface, as was shown before, are the pores more than 70 nm, critical cell fate level. To compare novel nanostructured surface of TMS with TNT, we analyze for both of the surface relatively large

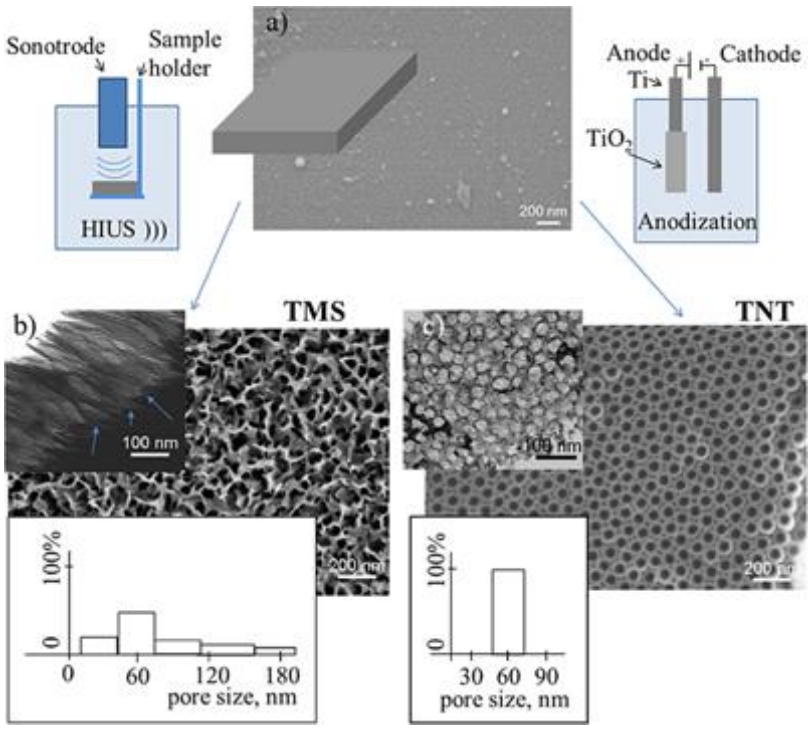

Figure 1. Schematic view of the two techniques used for titanium surface nanostructuring for following nanotopography-guided cell behavior and a view of the corresponding resulting surfaces formed by modification of initial flat titanium surface (shown in (a)); SEM of the sonochemically formed under high-intensity ultrasonic treatment (HIUS) titania mesoporous sponge layer (TMS) (b) and anodized titania nanotubes layer (TNT) (c). Insets (b, c) are TEM (slice-microtome) images of a cross-section through the TMS interface, side view (b), through the TNT, top view, and histograms of pore size distribution on TMS and TNT.

nanopores, 40–70 nm, to be close to fate level of TNT to see either TMS fate level is different. Indeed, our assumption, that for disordered TMS cell fate level is higher. Ultrasonication is known to produce surface modifications, including mechanical damage, through high-speed liquids jets, and shockwaves generated upon the asymmetric collapse of cavitation bubbles near a surface.[12] These mechanical effects have been considered by many as negative, as they may give rise to significant erosion and abrasion, such as cavitation damage on ship propellers and artificial heart valves.[13] However, the mechano-chemical effect of cavitation has been shown to be useful for practical applications in the modification of solid surfaces (roughening, cleaning, and formation of metal sponges), using liquids as benign as water.[14]

In the case of metals, the local conditions achievable under ultrasonic treatment etch and oxidize the surfaces leading to the formation of up to 300-nm-thick sponge-like crystalline surface layers, well-adhered to the bulk metal.[10] The TMS layer produced under ultrasonic treatment on Ti, shown in Figure 1b (inset), has high adhesion to the bulk metal. The surface metal sponge covered with oxide layer is porous, has a high surface area, and is covered by active OH-groups. Furthermore, such sponges combine the beneficial properties of metals with

a porous structure to give unique physical and mechanical properties such as low density, high surface-to-volume ratio, high thermal shock resistance, and high specific strength.[14] Moreover, the shape of the sonotrode can be adjusted for particular applications and allows easy modifications of large surface areas, as well as micron scale surface patterning.[15]

In order to compare the role of surface nanotopography for cell behavior only and not the effect of surface chemistry, we anneal all three types of compared surfaces, Ti, TMS, and TNT, at 450 °C for 3 h after surface modification to remove any organic contamination and to form a surface anatase oxide layer as confirmed using Raman spectroscopy (data not shown). In the case of TNT samples, heating the samples after anodization is an important technological step[6] to crystallize the oxide layer and burn difficult to remove residual organic components, remaining in the pores. In the case of TMS, the surface is already covered with a partially crystalline oxide layer immediately after treatment, due to the high local temperature that is achieved by the high-intensity ultrasonic treatment. In our case, resulted annealed layers have peaks of just anatase. Concerning TMS layer which already has some partial crystalline before annealing, annealing at 450 °C results also in anatase structure, however, not shown in this paper, some condition of initial sonication can further result in rutile. In following, it can be in focus how surface photoactivity which is different for different crystalline modification of titania, effect cell growth under the same surface morphology.

The hydrophilicity for both treated samples (TNT and TMS) was found to be very high, upon initial wetting, with a contact angle of 5.4° ± 0.8° for TNT and 5.2° ± 0.7° for TMS; after 5 min, the contact angle was 0.0° ± 0.0° ($p = 0.05$) for both samples, compared to the initial unmodified sample where the contact angle was 80° ± 2°. Besides, the common characteristics of surface chemistry and porous topography, TMS and TNT surface have different pore orientations: semi-ordered in the case of TNT and disordered in the case of TMS focusing the present study on the difference between ordered and disordered surfaces, with straight and random sided walls. Ions presented in the solution during porous structures development can dope titania layer. It is very interesting question, effect of doped ions from electrolyte to cell behavior. In the presented case of TMS, we treated in solution of NaOH. Other solutions with different ion size and ability to go into structure of TMS can be used, e.g. LiOH, KOH. Morphology of TMS is not effected with type of cation and is similar, presented in Figure 1 for TMS. The effect for following cell growth of Li^+, Na^+, K^+ was in the statistical error, not detectible. However, not shown in this paper, different cations size results in doping of titania and drastically change photoactivity of the surface, which can be used in following to guide cell migration with different efficiency for lab-on-chip application.

Interactions between biomaterials and host tissues are controlled by nanoscale features because of the three main reasons: cells grow on nanostructured extracellular matrices; biological events (signaling, cell–substrate interactions) occur at the nanometric level; adsorbed proteins and their aggregates are a few nanometers in dimension. In the paper, three biomaterial substrates (Ti, TMS, TNT) are at nanoscale different in the following morphological parameters: i) in surface roughness, ii) in pore size, and iii) in regularity of the nanopore arrangement. Each of these three parameters can critically control cell behavior. Meaningful comparisons can be drawn with studies that have used a similar surface modification technique (i.e., anodic oxidation or sonochemical modification), since although the surface roughness may be identical, but the physicochemical characteristics of the surface (wettability, surface energy, etc.) can be completely different. In our case, we have shown that TMS is unique and have higher critical fate rate in comparison with TNT, which is in focus of this paper, however, in the following the focus can be as was suggested, for example, to detailed comparison of just sonochemically formed TMS from different solutions, such as LiOH, NaOH, KOH, and CsOH. The formation of the same nanotopography can allow to go deeper into understanding the effect of ions for cell behavior on the surface as well as surface photoactivity. To move to the direction of just TMS before, it is idea to see it in comparison with well characterized and described in the literature TNT to have idea of its effect to cell. Thus, for TMS and TNT the first parameter i) surface roughness was Ra ≈ 30 nm which is higher to vacuum-deposited layer of titan after its thermal oxidation (Ra ≈ 5 nm). Critical to compare TMS and TNT are two other parameters ii) in pore size, and iii) in regularity of the nanopore arrangement. ii) Average pore size is comparable for TMS and TNT ≈ 70 nm, however, for TNT it is very narrow pore size distribution and for TMS it is much broader due to also the iii) parameter: regularity of the nanopore arrangement. Taking together it is expected that i) roughness effect positively to TNT and TMS in comparison with initial thermal-treated titania; ii) cells on ≥70 nm on TNT have been reported to be less effective in cell adhesion and proliferation, however, here we are interested in use of porosity 40–70 nm for following drug delivery and to find the system where pore size ≥70 nm can be fine for the cell, from this point TMS was expected to be better that TNT due to broad size distribution; iii) unregularly TMS structure in comparison with TNT should be also more preferable for the cells.

To test the surfaces, we employed C2C12 cells as a model cell line which is capable of differentiating along several lineages and is used as a model system for osteogenic and myogenic differentiation.[16] We first investigated C2C12 cell adhesion and proliferation on different surfaces (**Figure 2**). Cells proliferated well on all of the surfaces, however, nanostructuring of Ti affected cell proliferation rates. For cells grown on the control titania and TMS surfaces, the cell density increased significantly with increasing culture time (Figure 2a,

b, c). The density of cells in the case of TNT was much lower in comparison to glass, titania, and TMS (Figure 2d). After 24 h, C2C12 cells on the Ti and TMS surfaces had reached a density of approx. 200 cells mm^{-2}, while cells on the TNT surfaces had reached a density of only 50 cells mm^{-2} (Figure 2e, f). No significant difference in the cell density was observed between Ti and TMS, suggesting a negligible effect of irregular porosity even above 70 nm size for cell viability and growth. After 48 h of culture, cells grown on the Ti and

TMS surfaces had further increased cell number to a similar extent, while hardly any

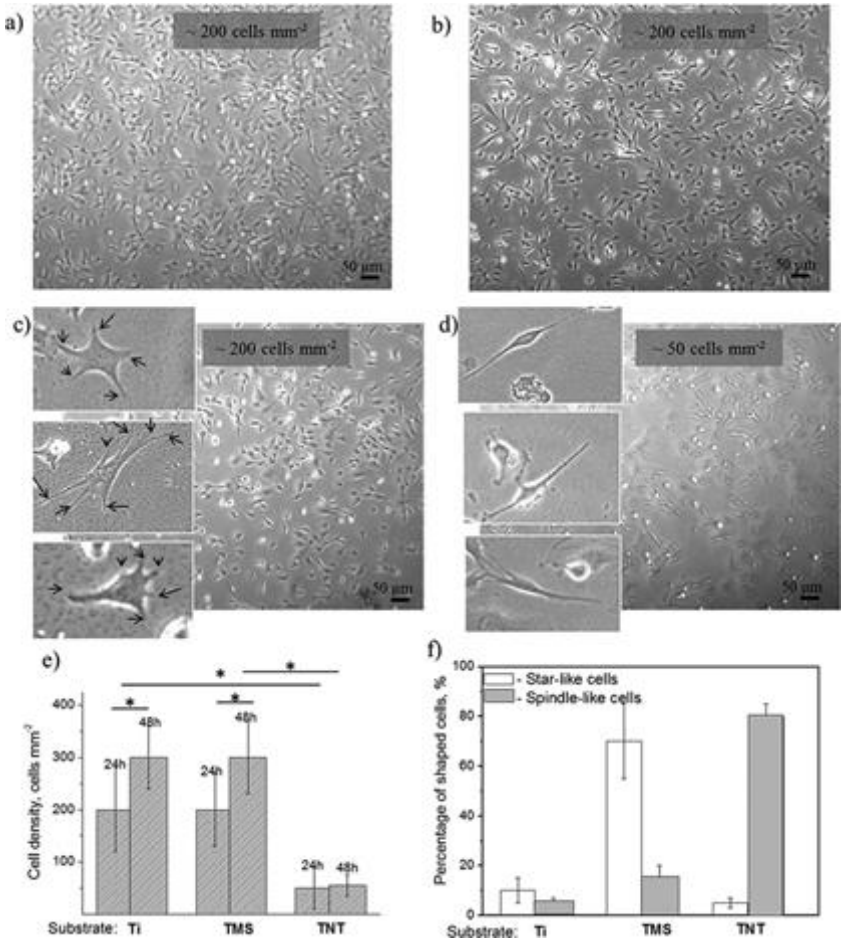

Figure 2. The representative optical micrographs after one day of C2C12 cell growth on different substrates: glass (a), unmodified titanium (b), sonochemically formed TMS (c), and TNT nanotubes formed by anodization (d). Insets depict individual cell morphologies on different surfaces, such as “star-like” in the case of TMS and spindle-like cell morphology in the case of TNT. (e) Cell density on different surfaces as culture time prolonged. (f) Quantification of the percentage of shaped cells on different surfaces after one day of culture. Bar charts represent means ± SD from three replicates each from three independent experiments. Comparison was done by ANOVA *$p < 0.05$.

proliferation for the TNT surfaces could be observed. The lower cell density on TNT surfaces might occur because the nanotubes are above 70 nm at which cell adhesion is hampered. In

all, there is a highly significant difference between TNT and the other two, but not between Ti and TMS.

Such size effects have been demonstrated by Paramasivam et al. who investigated mesenchymal stem cells on smooth (equivalent to Ti) and 70–100 nm TNT surfaces.[7] They showed that in the case of oriented pores, a pore spacing less than 30 nm accelerated integrin clustering and focal contact formation and strongly enhances cellular activities compared to smooth surfaces.[7]

Despite these studies would suggest[7] that TNT surfaces at these larger spacings would be less preferable for cells in comparison to unmodified Ti, there is no information concerning the response of cells to disordered TMS surfaces with similar average spacing. Interestingly, our experimental results show that TMS surfaces at these length scales show no reduction in proliferation, which could mean that the mean above a certain size for cell response on disordered random-sided walls TMS is above than that for ordered straight-sided walls TNT.

Cells on different nanostructured surfaces also exhibited a distinct morphology (Figure 2f). On TMS most cells adopted a star-like morphology (shown in inset in Figure 2c), while cells grown on TNT rather exhibited an elongated spindle-like appearance (shown in inset in Figure 2d), indicating that nanotopography influences the morphology of adherent cells. The cells on the control surface were also more flattened, measured by 3D confocal microscopy. In comparison, star-like cells on TMS and spindle-like cells on TNT could be a result of the interspersed pattern of adhesion on a rough surface.

In addition to cell proliferation, we further examined focal adhesion (FA) formation and cytoskeletal structures after 24 h of C2C12 cells growth on different substrates (**Figure 3**). To analyze cytoskeletal structures, we performed immunofluorescent staining for actin fibers and focal adhesions using phalloidin or α-vinculin antibody, respectively. Immunofluorescent analysis of cell populations on the untreated and nanostructured substrates revealed pronounced differences in focal adhesion (FA) formation and cytoskeletal structures (Figure 3). We quantified the total vinculin area and the number of FAs, each normalized to cell area, and observed significant differences ($p < 0.05$) between untreated and nanostructured surfaces. Although TMS did not induce detectable cytotoxic effects, still fewer focal adhesions were observed and these were largely restricted to one edge of the cell membrane. The same effect was seen in the case of TNT. This can be explained through the hypothesis raised by Paramasivam et al.[7] which suggests that vitality, proliferation, and

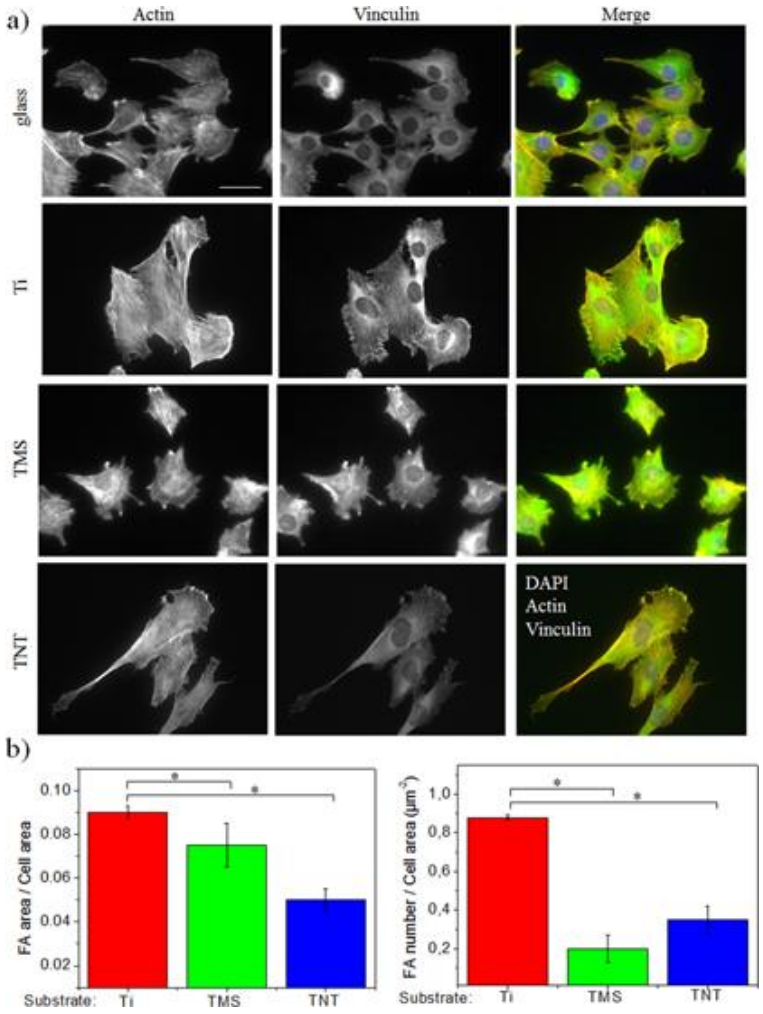

Figure 3. Evaluation of effect of titanium nanostructuring on cell morphology and FA formation of C2C12 cells at day 1 after plating. Scale bar, 50 µm. Cells were stained for actin using phalloidin and vinculin using a specific antibody; nuclei were counterstained with DAPI. Quantitative analysis of FA formation of C2C12 cells: total FA area per cell and the number of FAs per cell area. Comparison was done by ANOVA $*p < 0.05$.

motility of cells are critically influenced by nanoscale titania surface topography with a specific response to nanotubes with diameters between 15 and 100 nm.

In summary, FA formation of C2C12 cells as well as the total FA area per cell area was greater for the cells plated on the unmodified Ti substrate as compared to those plated on the nanostructured TMS and TNT. At the same time cells grown on TNT exhibited significantly lower proliferation rates, whereas cells on TMS and Ti showed comparable proliferation rates.

Cytoskeletal structure was also different and depended on surface nanotopography. In particular, we compared the nanotopography of titania and TMS samples (**Figure 4**a). For cells grown on both unmodified and nanostructured TMS, bundles of actin filaments, so-

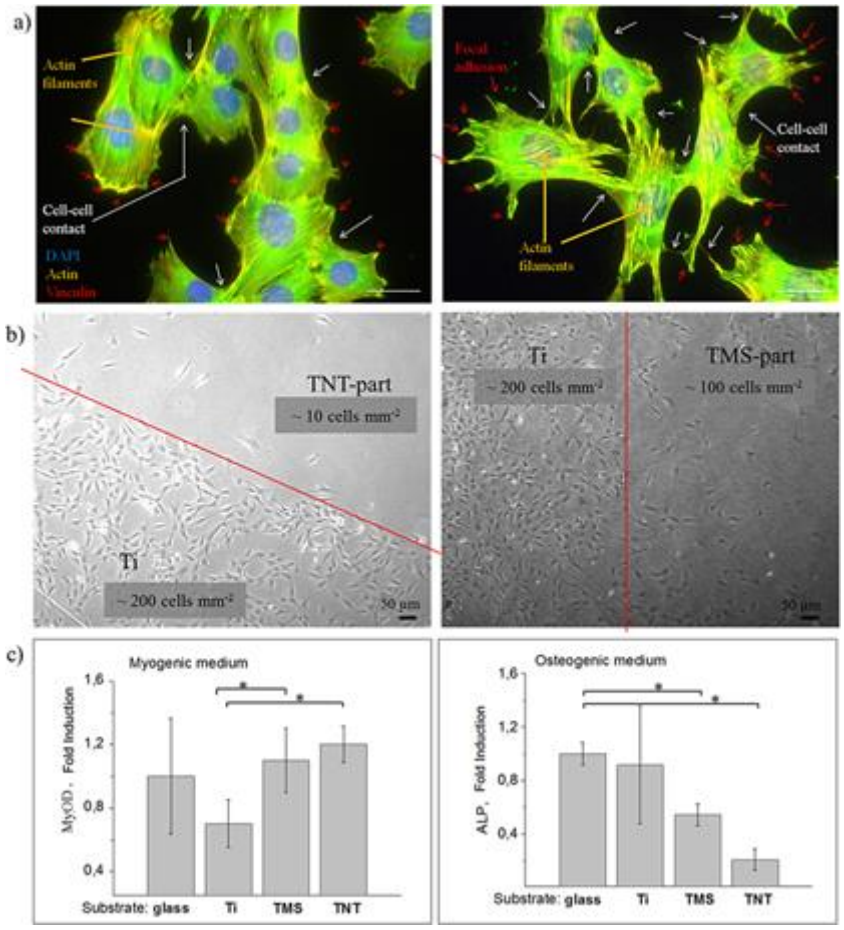

Figure 4. (a) Immunofluorescent analysis on cell morphology on different titanium nanostructures. Cells were stained for actin using phalloidin and vinculin using a specific antibody; nuclei were counterstained with DAPI. Areas of cell–cell interactions are indicated by white arrows, focal adhesion (FA) by red arrows. Images depict morphological structures between regularly shaped cells in the case of Ti (a-left) and "star-like" shaped cells on TMS (a-right), scale bar, 50 µm. (b) Brightfield microscopic analysis of C2C12 cells grown on surfaces with a nanostructuring patterning approach. Materials exhibit two structurally different areas, one representing a titanium-nanostructured titanium surface just adjacent to an unmodified titanium surface (c) Gene expression analysis by qRT-PCR to determine C2C12 differentiation capacity on different titanium surfaces. MyoG is a myoblast-specific transcription factor whereas ALP is an enzyme, which plays a crucial role during osteogenic differentiation. The error bars indicate standard deviations from mean values of three biological replicates ($n = 3$). Asterisks indicate statistical significance $*p < 0.05$.

called stress fibers, could be observed. However, stress fiber formation on the control titania was more pronounced in comparison to TMS, and fibers were longer and more uniformly distributed. Moreover, differences in cell morphology and cytoskeletal structure also affected cell–cell contacts.

Besides biological gradients, pore gradients are an attractive approach to guide cell behavior, offering a great potential for spatially controllable cell growth in implants for tissue engineering.[17] They would also be useful in the development of single-cell platforms to

screen the best nanoscale architectures for the desired response of a specific cell type. Toward this aim, we also engineered surfaces nanostructured on one side, while leaving the other half surface unmodified (Figure 4b). We observed a dramatically lower cell number on the half with a TNT surface as compared to flat titania on the other half-surface (Figure 4b, left). TMS also affected cell attachment and growth (Figure 4b, right) as compared to titania. The results demonstrate that a surface that exhibits two different nanostructured areas next to each other could have a direct influence on the growing preference of cells on the same substrate, opening up bioengineering lab-on-chip possibilities. It is interesting that together with step-like gradient in cell response to nanotopology, cells also have the same tendency (see also Figure 2) with respect to shape, being spindle-like on TNT, and “star-like” on TMS the sides of the surfaces.

We further tested the ability of C2C12 cells to differentiate along two mesenchymal lineages, the myogenic and osteogenic lineages (Figure 4c). We thereby observed that the nanostructure of the material has an impact on the osteogenic differentiation while it only moderately affects myogenic differentiation. On all surfaces, C2C12 cells clearly differentiate toward the myogenic lineage, characterized by the induction of MyoD, a major myogenic transcription factor that controls the early steps of myogenesis.[18] Conversely, during osteogenic differentiation triggered by 30 nM BMP-2, myotube formation was inhibited on all surfaces (images not shown) but osteogenic differentiation, characterized by the production of ALP was markedly different on nanostructured surfaces. Expression of alkaline phosphatase (ALP), an osteogenic marker, involved in matrix mineralization,[19] exhibited the highest expression on unmodified titanium and glass surfaces. Expression in cells differentiated on modified surfaces was much lower, showing the weakest expression on TNT surfaces. Similar trends were observed in other gene expression experiments (data not shown). However, when comparing TNT and TMS surfaces, BMP2-induced (30 nM) osteogenic differentiation was stronger on TMS than on TNT surfaces, highlighting again their potential for implant coatings and bone tissue engineering approaches. Our message is that osteogenic indeed is not too different for TNT, TMS, Ti thus one can think to use the structure for implantation, especially if additional functionality would be added, e.g., drug delivery due to porous structure. Moreover for lab-on-chip application, it is important to note that myogenic differentiations of TMS and TNT are significantly different from Ti, probably due to different initial shape of the adhered cells.

Taken together, we analyzed the prospects of ultrasonically formed mesoporous sponge layer (TMS), to guide cell behavior in comparison to flat titania and TNT, an anodized titania surface. The taking into account parameters to compare are i) surface roughness, is comparable for TNT and TMS and is higher to vacuum-deposited layer of titan after its thermal oxidation. Thus, this parameter is not one to explain the shown difference between TNT and TMS. Critical to

compare TMS and TNT are two other parameters ii) pore size, and iii) in regularity of the nanopore arrangement. ii) Average pore size is comparable for TMS and TNT ≈ 70 nm, however, for TNT it is very narrow pore size distribution and for TMS it is much broader due to also the iii) parameter: regularity of the nanopore arrangement. i) The roughness effect positively to TNT and TMS in comparison with initial thermal-treated titania; ii) cells on ≥70 nm on TNT have less effective in cell adhesion and proliferation, however, TMS system the srytical fate size for cell is higher; iii) unregularly TMS structure in comparison with TNT can also be the factor to increase critical for cell fate pore size for higher values on TMS versus TNT and explain significantly higher proliferation on titania and the disordered TMS surface as compared to TNT. The critical value for TNT surface, as was shown before, is the pores more than 70 nm, critical cell fate level. To compare novel nanostructured surface of TMS with TNT, we analyze for both of the surface relatively large nanopores, 40–70 nm, to be close to fate level of TNT to see either TMS fate level is different. Indeed, our assumption, that for disordered TMS cell fate level is high, supported with our observation, presented in the paper. Other important point is if any novel nanostructuring methodic is suggested, one should compare it with already existing well-studied nanotopographies to go further for details of one particular methodology. Thus in our case, we present promise TMS together to, well established, TNT and in following can take attention to have careful control of just one factor, for example, sonochemical treatment for TMS in different solutions, such as LiOH, NaOH, KOH, and CsOH, under the same pH, resulting of same nanotopography, but different photoactivity; or different roughness of the surface formed in NaOH if take different sonication treatment time of Ti. Furthermore, nanostructure influenced the capacity of C2C12 cells to differentiate, showing that nanotopography plays also an important role during cell differentiation of other cell types, which should be considered in tissue engineering strategies. In addition, a surface that exhibits two different nanostructured areas in close proximity opens opportunities to design cell culture platforms for controlled cell growth. The open pore structure of TMS and TNT can be loaded with chemical moieties, thus the possibility of both topographical and chemically directed cell growth and migration is attractive in future. Still, TMS surfaces allow immobilization of proteins and large molecular compounds while maintaining basal osteogenic differentiation capacity.

Experimental section

Preparation of Nanostructured Ordered and Disordered Surfaces

Glass- or ITO-coated glass substrates with a vacuum-deposited titanium layer (99.9%) were used. For TMS preparation, the Ti-glass substrates were ultrasonically treated in 5 M NaOH (Sigma–Aldrich) at 80%-intensity with an UIP1000hd (Hielscher Ultrasonics) operated at

20 kHz with a maximal output power of 1 000 W. Samples were placed into teflon home-made holder at 1 cm distance perpendicular to sonotrode. For TNT preparation, the Ti–ITO–glass samples were anodized in an aqueous solution of ethylene glycol (2 vol% water) containing 0.75 wt% NH_4F. At beginning of the anodizing, potential linearly increased from 0 to 40 V, than the anodizing performed at potentiostatic (40 V) mode till the total oxidation of a titanium layer on ITO. All samples were washed in ethanol and water. After washing, the structures were annealed at 450 °C in air. Milli-Q water was used in all aqueous solutions.

ITO were chosen as model substrate to have transparent surface for in situ monitoring of the cell behavior with optical microscopy to make staining and gene expression in certain moment of cell growth and to compare different cell number in time with optical microscopy. Moreover, the transparent surface to guide cell behavior is on high priority for lab-on-chip development. We did control experiments to prove that critical to guide cells is surface layer which depends on either Ti nanostructuring or nanostructuring of the layer on any enough inert substrate as, for example, Ti layer deposited in vacuum on glass, ITO surface and structured with different methods, e.g., sonochemical and electrochemical for our particular case.

Characterization Methods

Scanning electron microscopy (SEM) measurements were conducted with a Gemini Leo 1550 instrument (Zeiss) at an operation voltage of 3 keV. Transmission electron microscopy (TEM) images were obtained on a Zeiss EM 912 Omega transmission electron microscope operating at 300 kV. The samples were ultramicrotomed (Leica EM FC6) and placed onto the copper grids coated with a carbon film. Raman spectrometry of the substrates was performed using a confocal Raman microscope (alpha300, WITec) equipped with a piezoscanner. A frequency-doubled Nd:YAG laser excitation (λ = 532 nm) was used in combination with a Nikon 60× objective. Contact angle was measured with an optical tensiometer Krüss G23 M.

Cell Culture

Mouse C2C12 myoblasts (ATCC CRL-1772) were used for functional assays. Cells were cultured as sub-confluent monolayers in growth medium, consisting of Dulbecco's modified Eagle's medium (DMEM) (Gibco BRL) supplemented with 10% heat-inactivated fetal bovine serum (FBS) (Sigma), 2 mM glutamine, and 1% penicillin/streptomycin (Gibco BRL) at 37 °C and 5% CO_2. Cellular number and morphology on different titanium surface were monitored by bright field microscopy and documented by light micrographs. The distinction between differentially shaped cells was done by visual analysis. Total cell numbers were determined by manual counting of cells per image section. The total number of star- or spindle-shaped cells

on each image section was counted manually by eye and normalized to the total cell count. In total, 10 image sections were analyzed for every surface type in each experiment.

Immunofluorescent Staining

For microscopy and imaging, immunofluorescent staining was performed. At the respective time point, cells were fixed with 4% paraformaldehyde in phosphate-buffered saline, quenched for 5 min in a 50 mM ammonium chloride and permeabilized with a buffered Triton-X-100 solution for 10 min. Slides were then thoroughly washed with PBS and blocked in 3% BSA in PBS for 1 h. Subsequently, samples were incubated overnight with an anti-vinculin antibody (Sigma V9131) (1:300 in PBS/BSA). After washing with PBS, the samples were incubated with an Alexa-Fluor 488 labeled secondary goat anti-mouse antibody (Life Technologies, A-11001) (1:300) for 1 h. After washing, the samples were stained for 20 min with phalloidin Alexa-Fluor 594 (Life Technologies, A12381) (1:100) followed by incubation with DAPI (1:2 000) for 5 min. All stainings were performed at room temperature, except for the incubation with anti-vinculin antibody overnight, when the samples were left at 4 °C. The stained samples were mounted with Fluoromount-G (Southern Biotech) in inverted position on glass slides and examined via epifluorescence microscopy (Zeiss Axiovert 200M or Olympus IX inverted microscope). For presentation and calculations, the images were adjusted for brightness and color with ImageJ software (http://rsb.info.nih.gov/ij/). Confocal images that clearly showed focal adhesions were selected for analysis. RGB color images were converted to eight-bit black and white images using the image color RGB split function so that focal adhesions appeared as the black pixels. Focal adhesions were defined using Image J software by setting an intensity threshold. Image processing was identical for all cells in the different experimental groups. The number of focal adhesions per cell was counted using the analyze particles function.

Gene Expression Analysis by qRT PCR

C2C12 cells were seeded on the different titanium surfaces and grown to confluency after 6 day. Cells were subsequently starved for 3 h in DMEM without FCS supplements and stimulated for 3 days in medium containing 2% FCS (myogenic differentiation) or 2% FCS and 30 nM BMP2 (osteogenic differentiation). After stimulation, cells were harvested and total RNA was isolated using NucleoSpin isolation kit (Macherey&Nagel, Germany). 500 ng of RNA was subjected to reverse transcription. qRT PCR was performed using a SybrGreen-based detection system (Power SYBR Green PCR Master Mix, Life Technologies) and cDNA amplification was performed in a StepOne Plus Real Time PCR System (Life Technologies). For all used primers, amplification efficiencies were determined and mean-normalized

expression (MNE) ratios using HPRT as reference gene were calculated using the $\Delta\Delta c_T$ method with efficiency correction.[20]

Statistical Analysis

Statistic calculations were generated using GraphPad Prism software (at www.graphpad.com/prism). Comparison of multiple groups was done three way analysis of variance (ANOVA) test in the case of cell density with pairwise multiple comparison procedures by Holm-Sidak method; and one way analysis (ANOVA) in the case of focal adhesion and gene expression. Data were normally distributed due to Normality Shapiro–Wilk test. A *p*-value smaller than 0.05 was considered statistically significant.

References

[1] a) M. J. Dalby, N. Gadegaard, R. O. C. Oreffo, *Nature Mater*. **2014**, *13*, 558.

[2] T. Sjostrom, L. E. McNamara, R. M. D. Meek, M. J. Dalby, B. Su, *Adv Healthcare Mater*. **2013**, *2*, 1285.

[3] M. J. Dalby, N. Gadegaard, R. Tare, A. Andar, M. O. Riehle, P. Herzyk, C. D. W. Wilkinson, R. O. C. Oreffo, *Nature Mater*. **2007**, *6*, 997.

[4] R. J. McMurray, N. Gadegaard, P. M. Tsimbouri, K. V. Burgess, L. E. McNamara, R. Tare, K. Murawski, E. Kingham, R. O. Oreffo, M. J. Dalby, *Nature Mater*. **2011**, *10*, 637.

[5] N. R. Blumenthal, O. Hermanson, B. Heimrich, V. P. Shastria, *Proc. Natl. Acad. Sci*. **2014**, *111*, 16124.

[6] E. V. Skorb, D. V. Andreeva, *Adv. Funct. Mater*. **2013**, *23*, 4483.

[7] I. Paramasivam, H. Jha, N. Liu, P. Schmuki, *Small* **2012**, *8*, 3073.

[8] J. Park, S. Bauer, K. Mark, P. Schmuki, *Nano Lett.* **2007**, *7*, 1686.

[9] A. M. Lipski, C. J. Pino, F. R. Haselton, I.-W. Chen, V. P. Shastri, *Biomaterials* **2008**, *29*, 3836.

[10] a) E. V. Skorb, D. G. Shchukin, H. Möhwald, D. V. Andreeva, *Nanoscale* **2010**, *2*, 722; b) D. V. Andreeva, D. V. Sviridov, A. Masic, H. Möhwald, E. V. Skorb, *Small* **2012**, *8*, 820; c) J. Gensel, T. Borke, N. Pazos-Pérez, A Fery, D. V. Andreeva, E. Betthausen, A. Müller, H. Möhwald, E. V. Skorb, *Adv. Mater*. **2012**, *24*, 985.

[11] a) E. V. Skorb, H. Möhwald, *Adv. Mater*. **2013**, *36*, 5029; b) E. V. Skorb, D. V. Andreeva, *Adv. Func. Mater*. **2013**, *23*, 4483; c) E. V. Skorb, H. Möhwald, *Adv. Mater. Inter*. **2014**, DOI: 10.1002/admi.201400237.

[12] L. Rayleigh, Philos. Magaz. Ser. 1917, 634, 94.

[13] G. Melan, A. Bellato, F. M. Susin, T. Bottio, V. Tarzia, V. Pengo, G. Gerosa, A. Bagno, *J. Heart Valve Dis*. **2013**, *22*, 828.

[14] a) E. V. Skorb, D. Fix, D. G. Shchukin, H. Möhwald, D. V. Sviridov, R. Mousa, N. Wanderka, J. Schäferhans, N. Pazos-Pérez, A. Fery, D. V. Andreeva, *Nanoscale* **2011**, *3*, 985; b) E. V. Skorb, H. Möhwald, T. Irrgang, A. Fery, D. V. Andreeva, *Chem. Comm*. **2010**, *46*, 7897; c) D. G. Shchukin, D. V. Andreeva, E. V. Skorb, H. Möhwald, in: Supramolecular Chemistry of Hybrid Materials (Ed: K. Rurack), Wiley-VCH, Weinheim, Germany **2010**.

[15] D. G. Shchukin, E. V. Skorb, V. Belova, H. Möhwald, *Adv. Mater*. **2011**, *23*, 1922. _[16] T. Katagiri, A. Yamaguchi, M. Komaki, E. Abe, N. Takahashi, T. Ikeda, V. Rosen, J. M. Wozney, A. Fujisawa-Sehara, T. Suda, *J. Cell Biology* **1994**, *127*, 1755.

[17] K. Kant, S. P. Low, A. Marshal, J. G. Shapter, D. Losic, *ACS Appl. Mater. Inter.* **2010**, *2*, 3447.

[18] T. L. M. Pohl, J. H. Boergermann, G. K. Schwaerzer, P. Knaus, E. A. Cavalcanti-Adam, *Acta Biomater*. **2012**, *8*, 772.

[19] T. Katagiri, A. Yamaguchi, M. Komaki, E. Abe, N. Takahashi, T. Ikeda T, V. Rosen, J. M. Wozney, A. Fujisawa-Sehara, T. Suda, *J. Cell Biol*. **1994**, *127*, 1755.

[20] K. J. Livak, T. D. Schmittgen, *Methods* **2001***, 25*, 402.

Appendix 2. Switching the stiffness of polyelectrolyte assembly by light to control behavior of supported cells

Sviatlana A. Ulasevich,[1] Nadzeya Brezhneva,[1] Yulia Zhukova,[1] Helmuth Möhwald,[1] Peter Fratzl,[1] Felix H. Schacher,[2] Dmitry V. Sviridov,[3] Daria V. Andreeva,[4] and Ekaterina V. Skorb*[1]

[1] Max Planck Institute of Colloids and Interfaces, 14424 Potsdam, Germany

[2] Friedrich-Schiller-Universität Jena, Institut für Organische Chemie und Makromolekulare Chemie, 07743 Jena, Germany

[3] Belarusian State University, Chemistry Department, 220030 Minsk, Belarus

[4] Physical Chemistry II, Bayreuth University, 95440 Bayreuth, Germany

* Corresponding author

This paper is published in Macromolecular Bioscience: Macromol. Biosci. 2016, 16, 1422 – 1431. Text and figures are reproduced with permission of John Wiley and Sons.

My Contribution: I performed titanium surface nanostructuring.

http://onlinelibrary.wiley.com/doi/10.1002/mabi.201600127/abstract

Appendix 3. Methodology

Methods for titanium surface nanostructuring

Sonochemical Method

For the production of mesoporous titania (TMS) samples, a titanium layer (99.9%) of thickness 400 nm was deposited on glass substrates by means of Electron Beam Physical Vapor Deposition method (EB-PVD). TMS were obtained by sonochemical treatment with high intensity ultrasound (HIUS) in alkali solution. The size of the substrates was approx. 1 x 1 cm^2 to fit the homemade Teflon sample holder used for HIUS. Prior to sonication, the metal plates were degreased with isopropanol and rinsed with Milli-Q water (18 MΩ·cm). Titanium plates were ultrasonically treated in presence of 5M NaOH using the ultrasonic processor UIP1000hd (Hielscher Ultrasonics GmbH, Germany) with a maximum output power of 1000 W. The apparatus was equipped with a sonotrode BS2d18 (head area 2.5 cm^2) and booster B2-2.2, magnifying the working amplitude 2.2 times. Sonication was performed at *ca.* 20 kHz and constant temperature of around 333 K monitored by the thermo sensor inserted into the working solution.

Anodic Oxidation

For the production of titania nanotubes (TNT), titanium layer (99.9%) of thickness 150 nm was deposited on ITO-coated glass substrates by means of the Electron Beam Physical Vapor Deposition method (EB-PVD). TNTs were obtained by electrochemical oxidation. For their preparation the Ti-ITO-glass samples were anodized in an aqueous solution of ethylene glycol (2 vol. % water) containing 0.75 wt. % NH_4F. At the beginning of the anodization, the potential was linearly increased from 0 to 40 V over a time of 5 minutes, than the anodization was performed using the potentiostatic (40 V) mode till the total oxidation of a titanium layer on ITO.

All samples were additionally rinsed with ethanol and water and heat treated at 450 °C in the oven for at least 3 hours. Bulk titanium or its alloys, although being very tough, can be used for modification. In our experiments with cell studies it is advantageous to use a nanoscale-thick Ti layer on a glass substrate rather than bulk titanium, since the optical observation of the cell growth requires transparent samples. After thermal treatment, the titania layer on glass is transparent enough to observe cell adhesion and growth on the surface. Closest to bulk titanium are thicker layers, 400 nm to 150 nm. Thus, as model we use a 400 nm deposited layer on glass or on silicon for further atomic force microscopy study.

Milli-Q water (18 MΩ·cm) was used in all aqueous solutions. As a control glass substrates were used.

Surface characterization methods

The specimen surface nanotopography was inspected by *scanning electron microscopy* (SEM; Gemini Leo 1550 instrument, Leo Elektronenmikroskopie GmbH, Germany) at an operating voltage of 3 keV. Surface roughness (R_a) and 3D roughness profiles of the surfaces were obtained with *atomic force microscopy* (AFM; Dimension, Bruker, Germany) and image analysis was performed with the Nanoscope V614r1 software. AFM measurements were carried out in air at room temperature in tapping mode with micro cantilevers OMCL-AC160TS-W (Olympus, Japan). Typical cantilever values: resonant frequency 300 kHz; spring constant 42 N/m. Atomic force micrographs of a scan size 3 x 3 µm were made on three different places on the sample. *Contact angle* was measured by the homemade system used in Chapter 2.

Cell culture model

A mouse calvarial preosteoblast cell line MC3T3-E1 was obtained from Ludwig Boltzmann Institute, Vienna, Austria. Preosteoblasts were maintained in normal culture medium α-MEM, supplemented with 10% (by volume) fetal calf serum (FCS), 4500 mg glucose, 0.1% (by volume) gentamycin, 0.1% (by volume) ascorbic acid under standard culture condition (37°C, 5% CO_2 in a humidified atmosphere). Cells were passaged in total three times every 24 hours by a dilution factor of 1/6. The media was refreshed every 48 h. After reaching confluence, cells were dissociated from culture vessels by incubating with pronase for 3 – 5 min. All surfaces and scaffolds were autoclaved before cell culture experiments.

Stainings and cell imaging techniques

Staining for cytoskeletal actin

Morphologies of MC3T3-E1 cells cultured on various surfaces were observed by *confocal laser scanning microscopy* (CLSM) and SEM. The cells were seeded onto surfaces at a density of 6000 cells/cm^2. Normal culture medium and standard conditions were employed. At respective time point after seeding, the cells were washed twice with phosphate-buffered saline (PBS). To prepare samples for CLSM observation, the cells were fixed with 4% paraformaldehyde in PBS, and permeabilized with buffered Triton-X100 (Sigma-Aldrich, Steinheim, Germany) for 10 min at room temperature. The scaffolds were then thoroughly washed with PBS and stained for 60-90 min with phalloidin Alexa488 (Invitrogen, Oregon, USA) (1:20) in dark at 4°C for cytoskeletal filamentous F-actin. After that scaffolds were thoroughly washed with PBS again,

and stained for nuclei with TO-PRO3 iodide (Invitrogen, Oregon, USA) (1:300) for 5 min at room temperature. The scaffolds were washed with PBS, mounted with Fluoro-Mount in inverted position on the glass slides, and examined via confocal microscopy (Leica Microsystems, Mannheim, Germany).

To prepare samples for SEM observation, the cells were fixed twice: primary fixation with 2.5% glutaraldehyde (in PBS) for 30 min and secondary fixation with 4% PFA for 20 min. Thereafter, the cells were dehydrated by gradient ethanol solutions (25%, 50%, 75%, 90% and 100%), each for 5 min. The treated samples were dried overnight in desiccator, sputter-coated with gold and observed using SEM.

Immunofluorescent Staining for Vinculin

MC3T3-E1 cells were seeded onto surfaces maintaining the seeding density and culture method as described above. Cell adhesion was evaluated by immunofluorescent staining of focal contacts. At 3h after seeding, cells were fixed with 4% paraformaldehyde in PBS, quenched for 5 min in 50 mM ammonium chloride and permeabilized with buffered Triton-X-100 solution for 10 min. Specimens were then thoroughly washed with PBS and blocked in 3% BSA (in PBS) for 1 hour. After that samples were incubated overnight with anti-vinculin antibody (Sigma V9131) (1:300 in PBS/BSA). After washing with PBS, samples were incubated with secondary goat anti-mouse antibody Alexa594 (Invitrogen) (1:300) for 1 hour. After washing, samples were stained for 20 min with phalloidin Alexa488 (Invitrogen) (1:100). The staining was performed at room temperature, except for the incubation with anti-vinculin antibody overnight, when the samples were left at 4°C. The stained samples were mounted with Fluoro-Mount in inverted position on thin glass slides and examined via confocal microscopy. Imaging was conducted by using a Leica confocal laser scanning microscope (Leica Microsystems, Mannheim, Germany). The samples were excited with the argon laser line at 488 nm and 594 nm for Phalloidin Alexa488 (actin stain) and Alexa594 (focal contacts stain), respectively. The images were captured with a PL FLUOTAR objective.

Cell Migration

In order to investigate migration characteristics of MC3T3-E1 cells, the scratch wound healing assay was performed using ibidi Culture-Inserts (Ibidi GmbH, Germany) according to the manufacturer's instructions. MC3T3-E1 cells were seeded to become confluent in 10% FCS α-MEM. 1 hour prior to insert removal, cells were incubated with 10 µg/ml mitomycin C to block cell proliferation. After insert removal, the wound closure was allowed to proceed and imaged by phase contrast microscopy. Pictures were taken using a 5× objective in bright field modus every 30 min for at least 16 h. Life cell imaging was performed within a heat and CO_2 controlled

Life Cell Imaging chamber (ibidi GmbH) using an automated sample table mounted on an Axiovert 200 M (Carl Zeiss, Jena, Germany) in combination with Axiovision Mark&Find tool.

The analysis of cell migration was performed with an automatic algorithm developed recently for analysis of cell migration in chemotaxis assays. This approach allows estimating migration characteristics such as mean migration speed, neighborhood analysis, and is able to distinguish between directed and random migration without a favored direction. In brief, the automatic tracking algorithm includes two main steps: segmentation and tracking. Firstly, the dense optical flow is computed to segment the foregrounds which are the cells. The cell nuclei are roughly segmented by an adaptive inverse threshold, and the cell bodies are approximated from the nuclei via watershed segmentation on the foreground mask. Thus, the position and the neighborhood are computed for each cell at each time point on time-lapse data. The neighborhood is here defined as cells with adjacent voronoi areas. The trajectories are computed by an overlap heuristic on the nuclei mask. The analysis was restricted on cells close to the scratch area.

List of Abbreviations

AFM	Atomic Force Microscopy
BSA	Bovine Serum Albumin
CLSM	Confocal Laser Scanning Microscopy
2D	Two-dimensional
3D	Three-dimensional
3D-MA	Three-dimensional matrix adhesion
EB-PVD	Electron Beam Physical Vapor Deposition
ECM	Extracellular matrix
ESEM	Environmental Scanning Electron Microscopy
FA	Focal adhesion
FbA	Fibrillar adhesion
FCS	Fetal Calf Serum
HA	Hydroxyapatite
HIUS	High Intensity Ultrasound
LbL	Layer-by-Layer
PBS	Phosphate Buffer Saline
PE	Polyelectrolyte
SEM	Scanning Electron Microscopy
TEM	Transmission Electron Microscopy
TMS	Mesoporous Titania
TNT	Titania Nanotubes

References

[1] X. Liu, P. K. Chu, C. Ding, *Mater. Sci. Eng., R* **2004**, *47*, 49.
[2] F. Variola, J. B. Brunski, G. Orsini, P. Tambasco de Oliveira, R. Wazen, A. Nanci, *Nanoscale* **2011**, *3*, 335.
[3] F. Variola, F. Vetrone, L. Richert, P. Jedrzejowski, J.-H. Yi, S. Zalzal, S. Clair, A. Sarkissian, D. F. Perepichka, J. D. Wuest, F. Rosei, A. Nanci, *Small* **2009**, *5*, 996.
[4] A. M. Ballo, A. Palmquist, O. Omar, W. Xia, *Dental Implant Surfaces - Physicochemical Properties, Biological Performance, and Trends*, INTECH Open Access Publisher, 2011.
[5] Y. Sasai, *Nature* **2013**, *493*, 318.
[6] M. E. Todhunter, N. Y. Jee, A. J. Hughes, M. C. Coyle, A. Cerchiari, J. Farlow, J. C. Garbe, M. A. LaBarge, T. A. Desai, Z. J. Gartner, *Nat Meth* **2015**, *12*, 975.
[7] K. L. Schmeichel, M. J. Bissell, *J. Cell Sci.* **2003**, *116*, 2377.
[8] https://www.hielscher.com/wire_01.htm.
[9] P. T. F. Swiergon, Juliana, P., Knoerzer, K., *2nd Meeting of the Asia-Oceania Sonochemical Society, Kuala Lumpur, Malaysia* **2015**, 41.
[10] J. Kopf, S. Ulasevich, O. Baidukova, Y. Zhukova, J. W. C. Dunlop, P. Fratzl, P. Rikeit, P. Knaus, S. K. Poznyak, D. V. Andreeva, E. V. Skorb, *Adv. Eng. Mater.* **2016**, *18*, 476.
[11] E. V. Skorb, A. V. Volkova, D. V. Andreeva, *Curr. Org. Chem.* **2014**, *18*, 2315.
[12] E. V. Skorb, O. Baidukova, A. Goyal, A. Brotchie, D. V. Andreeva, H. Mohwald, *J. Mater. Chem.* **2012**, *22*, 13841.
[13] M. Delcea, H. Möhwald, A. G. Skirtach, *Adv. Drug Delivery Rev.* **2011**, *63*, 730.
[14] E. V. Skorb, H. Möhwald, *Adv. Mater.* **2013**, *25*, 5029.
[15] E. V. Skorb, H. Möhwald, *Adv. Mater. Intefaces* **2014**, *1*, 1400237.
[16] D. G. Shchukin, E. Skorb, V. Belova, H. Möhwald, *Adv. Mater.* **2011**, *23*, 1922.
[17] D. V. Andreeva, D. V. Sviridov, A. Masic, H. Möhwald, E. V. Skorb, *Small* **2012**, *8*, 820.
[18] D. V. Andreeva, D. Fix, H. Mohwald, D. G. Shchukin, *Adv Mater* **2008**, *20*, 2789.
[19] E. Skorb, D. Shchukin, H. Möhwald, D. Andreeva, *Langmuir* **2010**, *26*, 16973.
[20] E. V. Skorb, L. I. Antonouskaya, N. A. Belyasova, D. G. Shchukin, H. Möhwald, D. V. Sviridov, *Appl. Catal., B* **2008**, *84*, 94.
[21] E. V. Skorb, D. V. Andreeva, A. P. Raiski, N. A. Belyasova, H. Mohwald, D. V. Sviridov, *Photochem. Photobiol. Sci.* **2011**, *10*, 1974.
[22] M. Rumpler, A. Woesz, F. Varga, I. Manjubala, K. Klaushofer, P. Fratzl, *Journal of Biomedical Materials Research Part A* **2007**, *81A*, 40.
[23] M. Rumpler, A. Woesz, J. W. C. Dunlop, J. T. van Dongen, P. Fratzl, *Journal of The Royal Society Interface* **2008**, *5*, 1173.
[24] C. M. Bidan, K. P. Kommareddy, M. Rumpler, P. Kollmannsberger, Y. J. M. Bréchet, P. Fratzl, J. W. C. Dunlop, *PLoS ONE* **2012**, *7*, e36336.
[25] C. M. Bidan, K. P. Kommareddy, M. Rumpler, P. Kollmannsberger, P. Fratzl, J. W. C. Dunlop, *Adv. Healthcare Mater.* **2013**, *2*, 186.
[26] Z. Nie, E. Kumacheva, *Nat Mater* **2008**, *7*, 277.
[27] V. Belova-Magri, A. Brotchie, C. Cairos, R. Mettin, H. Mohwald, *ACS Appl Mater Interfaces* **2015**, *7*, 4100.
[28] V. Belova, D. A. Gorin, D. G. Shchukin, H. Möhwald, *Angew. Chem. Int. Ed.* **2010**, *49*, 7129.
[29] V. Belova, D. A. Gorin, D. G. Shchukin, H. Mohwald, *ACS Appl Mater Interfaces* **2011**, *3*, 417.
[30] V. Belova, D. G. Shchukin, D. A. Gorin, A. Kopyshev, H. Mohwald, *PCCP* **2011**, *13*, 8015.
[31] T. J. Mason, J. P. Lorimer, *Applied sonochemistry: the uses of power ultrasound in chemistry and processing*, Wiley-VCH, 2002.
[32] A. Sandá, V. García Navas, O. Gonzalo, *Materials & Design* **2011**, *32*, 2213.
[33] K. Kant, S. P. Low, A. Marshal, J. G. Shapter, D. Losic, *ACS Appl. Mater. Interfaces* **2010**, *2*, 3447.
[34] J. Yan, F. Zhou, *J. Mater. Chem.* **2011**, *21*, 9406.

[35] J. M. Macak, H. Tsuchiya, A. Ghicov, K. Yasuda, R. Hahn, S. Bauer, P. Schmuki, *Curr. Opin. Solid State Mater. Sci.* **2007**, *11*, 3.
[36] S. Yoriya, *International Journal of electrochemical science* **2012**, *7*, 9454.
[37] W. H. Ziegler, R. C. Liddington, D. R. Critchley, *Trends in cell biology* **2006**, *16*, 453.
[38] R. Pankov, A. Momchilova, in *Advances in Regenerative Medicine: Role of Nanotechnology, and Engineering Principles: Role of Nanotechnology, and Engineering Principles*, 10.1007/978-90-481-8790-4_1 (Eds: V. P. Shastri, G. Altankov, A. Lendlein), Springer Netherlands, Dordrecht 2010, 1.
[39] S. Stehbens, T. Wittmann, *Methods in cell biology* **2014**, *123*, 335.
[40] Y. Ho, S.-H. Kok, J.-S. Wang, L.-D. Lin, *Journal of Biomedical Materials Research Part A* **2014**, *102*, 1187.
[41] L. Saldaña, N. Vilaboa, *Acta Biomater.* **2010**, *6*, 1649.
[42] J. T. Parsons, A. R. Horwitz, M. A. Schwartz, *Nature reviews. Molecular cell biology* **2010**, *11*, 633.
[43] D. J. Webb, J. T. Parsons, A. F. Horwitz, *Nat Cell Biol* **2002**, *4*, E97.
[44] A. D. Doyle, F. W. Wang, K. Matsumoto, K. M. Yamada, *The Journal of Cell Biology* **2009**, *184*, 481.
[45] X. Chen, O. Nadiarynkh, S. Plotnikov, P. J. Campagnola, *Nat. Protoc.* **2012**, *7*, 654.
[46] H.-J. Butt, B. Cappella, M. Kappl, *Surf. Sci. Rep.* **2005**, *59*, 1.
[47] E. Cukierman, R. Pankov, D. R. Stevens, K. M. Yamada, *Science* **2001**, *294*, 1708.
[48] E. Cukierman, R. Pankov, K. M. Yamada, *Curr. Opin. Cell Biol.* **2002**, *14*, 633.
[49] J. Domke, S. Dannöhl, W. J. Parak, O. Müller, W. K. Aicher, M. Radmacher, *Colloids and Surfaces B: Biointerfaces* **2000**, *19*, 367.
[50] E. Takai, K. D. Costa, A. Shaheen, C. T. Hung, X. E. Guo, *Annals of Biomedical Engineering* **2005**, *33*, 963.
[51] H. W. Wu, T. Kuhn, V. T. Moy, *Scanning* **1998**, *20*, 389.
[52] A. Krause, E. A. Cowles, G. Gronowicz, *J. Biomed. Mater. Res.* **2000**, *52*, 738.
[53] K. P. Kommareddy, C. Lange, M. Rumpler, J. W. Dunlop, I. Manjubala, J. Cui, K. Kratz, A. Lendlein, P. Fratzl, *Biointerphases* **2010**, *5*, 45.
[54] S. A. Ulasevich, S. K. Poznyak, A. I. Kulak, A. D. Lisenkov, M. Starykevich, E. V. Skorb, *Langmuir* **2016**, *32*, 4016.
[55] S. A. Ulasevich, N. Brezhneva, Y. Zhukova, H. Mohwald, P. Fratzl, F. H. Schacher, D. V. Sviridov, D. V. Andreeva, E. V. Skorb, *Macromol Biosci* **2016**, 10.1002/mabi.201600127.